HHS Public Access

Author manuscript

AJR Am J Roentgenol. Author manuscript; available in PMC 2024 June 25.

Published in final edited form as:

AJR Am J Roentgenol. 2024 January ; 222(1): e2329933. doi:10.2214/AJR.23.29933.

Update on DWI for Breast Cancer Diagnosis and Treatment Monitoring

Roberto Lo Gullo, MD[1], **Savannah C Partridge, PhD**[2], **Hee Jung Shin, MD**[3], **Sunitha B Thakur, PhD**[1,4], **Katja Pinker, MD, PhD**[1]

[1]Department of Radiology, Memorial Sloan Kettering Cancer Center, New York, NY 10065, USA

[2]Department of Radiology, University of Washington School of Medicine, University of Washington, Seattle, WA, USA 98109, USA

[3]Department of Radiology and Research Institute of Radiology, Asan Medical Center, University of Ulsan College of Medicine, Seoul 05505, South Korea

[4]Department of Medical Physics, Memorial Sloan Kettering Cancer Center, New York, NY 10065, USA

Abstract

DWI is a noncontrast MRI technique that measures the diffusion of water molecules within biologic tissue. DWI is increasingly incorporated into routine breast MRI examinations. Currently, the main applications of DWI are breast cancer detection and characterization, prognostication, and the prediction of treatment response to neoadjuvant chemotherapy. In addition, DWI is promising as a noncontrast MRI alternative for breast cancer screening. Problems with suboptimal resolution and image quality have restricted the mainstream use of DWI for breast imaging, but these shortcomings are being addressed through several technologic advancements. In this article, we present an up-to-date review on the use of DWI for breast cancer imaging, including a summary of the clinical literature and recommendations for future use.

Introduction

Dynamic contrast-enhanced (DCE) MRI allows for malignant breast lesions to be visualized on account of their neovascularity. DCE MRI has the highest sensitivity for breast cancer detection among current clinical imaging modalities but is hindered by moderate specificity and reliance on the administration of a contrast agent, resulting in additional time and costs as well as risks of adverse events [1, 2]. In this setting, DWI has emerged as an alternative noncontrast MRI technique for detection of breast malignancy.

DWI is a fast technique, typically involving only 2−3 minutes of scan time, reflecting the diffusion of water molecules within biologic tissue. Substantial evidence indicates that DWI provides useful quantitative and qualitative information regarding malignant breast lesions. Thus, DWI is increasingly incorporated within clinical breast MRI examinations

Corresponding author: Katja Pinker MD, PhD, pinkerdk@mskcc.org, Department of Radiology, Memorial Sloan Kettering Cancer Center, New York, NY 10065, USA.

as a supplemental technique for multiple indications, including lesion detection and characterization, prognostication, and prediction of treatment response to neoadjuvant chemotherapy (NAC) [3]. Noncontrast screening breast MRI based on DWI is also under investigation [3, 4].

In this article, we present an up-to-date review on the use of DWI for breast cancer imaging, including a summary of the clinical literature and recommendations for future use. We will cover the basics of DWI, current clinical applications of DWI in breast cancer diagnosis and treatment response assessment, emerging clinical applications of DWI in screening, advanced artificial intelligence (AI) modeling incorporating DWI, technical challenges in the clinical implementation of DWI, emerging advanced acquisition techniques, and efforts in DWI standardization.

Basics of DWI

DWI is a noncontrast MRI technique reflecting intrinsic tissue contrast related to the diffusion of water molecules within biologic tissue. It is commonly applied in neurologic and prostate imaging, and is widely available across various MRI systems. As the diffusion of water molecules is influenced by many factors (e.g., cell membrane integrity, cell density, and tissue microstructure), DWI is reflective of the cellular microenvironment.

The signal intensity on DWI is inversely proportional to the mobility of water molecules, as described by the general monoexponential decay equation:

$$S_D = S_0 e^{-b * ADC} \quad [1]$$

where S_D represents signal intensity on DWI, S_0 represents signal intensity without diffusion weighting, b represents the diffusion sensitization factor determined by diffusion gradients' strength and timing (s/mm^2), and ADC represents the diffusion rate determined by the mean area traversed by a molecule of water per unit of time (mm^2/s). ADC maps are constructed using DW images acquired at two or more b-values. Malignant lesions typically exhibit hindered water diffusion and lower ADC on DWI due to their high cellularity compared with benign and healthy tissue [3, 4] (Fig.1) [5–7].

Current Clinical Applications

Discrimination Between Benign and Malignant Breast Lesions

Numerous studies have demonstrated that multiparametric MRI (mpMRI) combining DWI and DCE MRI improves the specificity and diagnostic accuracy of breast lesion characterization, thereby reducing unnecessary biopsies of benign lesions (Fig. 2). Indeed, a meta-analysis [8] of 14 studies (1140 patients with 1276 breast lesions) showed that mpMRI combining DCE MRI and DWI yielded superior diagnostic accuracy to either DCE MRI or DWI alone. The pooled sensitivity, specificity, and area under the summary ROC (SROC) curve for mpMRI were 91.6%, 85.5%, and 0.94, compared to 93.2%, 71.1%, and 0.85 for DCE MRI alone.

To further improve the diagnostic performance of mpMRI combining DCE MRI and DWI, a phase II trial by the Eastern Cooperative Oncology Group-American College of Radiology Imaging Network (ECOG-ACRIN) Cancer Research Group (A6702) [9] involving 67 patients with 81 MRI-detected lesions showed that implementing an ADC threshold of 1.53×10^{-3} mm^2/s within an mpMRI framework reduced the biopsy rate by 20.9% while maintaining the level of sensitivity. These findings were confirmed in a multi-center retrospective study by Clauser et al. [10] involving 657 patients with 696 lesions assessed as BI-RADS category 4 (i.e., suspicious lesions) according to the American College of Radiology BI-RADS, where applying an ADC cutoff of $\geq 1.5 \times 10^{-3}$ mm^2/s to de-escalate lesion recommendations (i.e., avoid biopsy) yielded a sensitivity of 96.6%, with a potential 32.6% reduction of unnecessary biopsies (92/282 benign biopsies). Additionally, per several meta-analyses, the added diagnostic value of DWI is independent of magnetic field strength and the ADC measurement method (whole-lesion measurement vs estimate in a single area), as well as robust to the administration of gadolinium-based contrast agents [11–13].

Data proving the efficacy of DWI and the ADC metric in lesion characterization are most clear for enhancing masses. On the other hand, in non-mass enhancement (NME) lesions, several studies have demonstrated a more limited role of DWI [9, 14–17]. For example, Marino et al. [17] evaluated 66 patients with suspicious NME lesions on DCE MRI (BI-RADS category 4 or 5) that were subsequently biopsied under MRI guidance, with DWI resulting in only a slightly increased specificity at the expense of sensitivity and overall diagnostic accuracy. Meanwhile, in the ACRIN 6702 trial, implementing an ADC cutoff significantly reduced unnecessary biopsies for masses but not for NME [9].

Recently, AI-enhanced mpMRI with DCE and DWI was explored for lesion classification with promising results. Dalmis et al. [18] used a dataset of 576 lesions including 368 biopsy-proven malignant lesions, 149 biopsy-proven benign lesions, and 59 lesions deemed benign based on follow-up findings. Imaging features were extracted from DCE and T2-weighted sequences and matched with ADC value, patient age, and BRCA genetic testing results to generate a lesion classification system. The AUC of the model based on DCE MRI alone was 0.811, but when all of the clinical information and the imaging information from DWI were added, the AUC increased to 0.85, producing 19 (12.8%) fewer false positives compared to radiologist review. Elsewhere, Feng et al. [19] extracted features from DCE MRI and DWI for lesion classification, achieving an accuracy of 85.0%, sensitivity of 84.6%, and specificity of 85.7%.

Breast Cancer Characterization

Recent studies have shifted their focus from breast cancer diagnosis (i.e., malignant vs. benign breast lesions) to breast cancer characterization and prognosis [20–23]. As DWI reflects tissue microstructure, quantitative ADC assessment may be used to differentiate tumor grades, proliferation rates, and subtypes, as well as to predict the upgrade of pure ductal carcinoma in situ (DCIS) to invasive cancer before surgical excision or to predict the likelihood of axillary involvement.

Studies have reported how DWI, particularly lower ADC values, can predict which DCIS lesions diagnosed on core-needle biopsy will have an upgraded diagnosis of invasive disease

on surgical excision [24–26]. Pure DCIS typically exhibits higher ADC values than invasive ductal carcinoma [27], likely due to its lower cellularity.

Studies have also reported how ADC values can distinguish between tumor grades, proliferation rates, and subtypes. For example, Costantini et al. [28] analyzed 162 malignant lesions in 136 patients, finding a significant inverse correlation between the ADC value and tumor grade. The mean ADC was higher in less aggressive and in situ cancers (1.19×10^{-3} mm^2/s) versus more aggressive cancers (0.96×10^{-3} mm^2/s). Choi et al. confirmed in a larger-scale study the difference in ADC values between in situ and invasive cancers and also found that lower ADC values were significantly associated with increased proliferation (Ki-67), estrogen receptor (ER) positivity, progesterone receptor (PR) positivity, and increased microvascular density [29]. Several other investigator groups also found that lower ADC values were associated with ER positivity [30–34]. Meanwhile, Horvat et al. [20] demonstrated that ADC values were significantly lower in luminal cancers compared to non-luminal cancers.

Elsewhere, regarding the value of DWI for prognostication, Razek et al. found lower ADC values in high-grade, larger-sized breast cancers and in cancers with positive lymph node metastases. Similarly, in a study by Kim et al. of 270 patients with early-stage invasive breast cancer, 58 of whom had axillary lymph node metastases, patients with nodal metastases had lower ADC values [35].

Although non-invasive breast cancers consistently present with higher or even borderline benign ADC values, ADC values are less consistent between different invasive molecular subtypes of breast cancers. More aggressive breast cancer such as HER2+ or triple negative breast cancer may have significant tumoral edema, artificially increasing ADC values. ROI measurement methods (e.g., whole-tumor vs hot-spot measurement) and the choice of ADC metric (e.g., minimum, maximum, mean) used may also be contributing factors [20].

The application of AI to DWI alone or to mpMRI for improved breast cancer characterization has yielded promising results. To improve non-invasive molecular subtyping, Leithner et al. first analyzed radiomic features extracted from ADC maps coupled with machine learning, showing that the differentiation of breast cancer subtypes with high accuracy was possible [21]. A follow-up study [36] confirmed that tumor subtypes carry distinct radiomic features, with the model achieving AUCs over 0.80 for differentiating triple negative and luminal A breast cancers from other subtypes. Meanwhile, Huang et al. [37] showed in 162 patients that a combined machine learning approach using radiomic features from DCE MRI, T2-weighted imaging, and ADC maps predicted not only the molecular subtype but also androgen receptor (AR) status—a biomarker associated with favorable disease-free survival and overall survival and which is also a potential therapeutic target. The model had the best performance for discriminating AR status, yielding an AUC of 0.907 and an accuracy of 85.8% in the testing dataset.

Additional studies incorporating AI have been performed to predict predictive and prognostic tumor features such as Ki-67 status and tumor grade. For example, Liu et al. [38] built an AI model to predict Ki-67 status using T2-weighted images, DWI, and DCE T1-

weighted images, achieving an AUC of 0.875. Similar results were reported by Zhang et al. [39], where the ADC-based radiomic model achieved an AUC of 0.72 and accuracy of 70% in the test set. Elsewhere, Fan et al. [40] evaluated DCE MRI- and DWI-based radiomics for the joint prediction of Ki-67 expression and tumor grade, achieving AUCs of 0.811 and 0.816, respectively. The authors published similar results [41] using super-resolution ADC images, whereby high-resolution images were produced from low-resolution images using bicubic interpolation and deep convolutional neural networks. Radiomic features extracted from super-resolution ADC images demonstrated slight improvements in AUC versus the original ADC images to predict Ki-67 expression (AUCs of 0.818 and 0.801, respectively) and tumor grade (AUCs of 0.826 and 0.828, respectively).

Assessment of Axillary Lymph Nodes

Several studies have focused on the use of DWI in the assessment of axillary lymph nodes to predict metastases. For example, in a study by Guvenc et al. [42] of 85 patients, the ADC values of the most suspicious ipsilateral lymph nodes were compared against the ADC values of contralateral benign axillary lymph nodes, with lymph nodes having a short-axial diameter of ≥ 1 cm. In that study, the mean ADC in metastatic lymph nodes was significantly lower than that for benign lymph nodes ($p < .0001$). Using a cutoff ADC value of 0.985×10^{-3} mm^2/s, the sensitivity, specificity, PPV, and NPV improved from 79%, 81%, 65% to 89%, to 83%, 98%, 95%, and 93%, respectively. Fardanesh et al. [43] attempted to define the best ADC metrics and threshold to differentiate benign from malignant lymph nodes in 217 patients. Although ADC values were significantly different between benign and malignant lymph nodes, there was also significant overlap. The best mean ADC threshold for axillary lymph nodes was 1.004×10^{-3} mm^2/s, which yielded accuracy of 75%, sensitivity of 71%, specificity of 79%, PPV of 77%, and NPV of 74%. That threshold is lower than the threshold of 1.300×10^{-3} mm^2/s recommended by the European Society of Breast Imaging (EUSOBI) for n-breast primary lesions, suggesting that the thresholds for breast tumors and axillary lymph nodes may differ.

Recently, radiomics has also been explored for assessment of axillary lymph nodes. Chai et al. [44] used mpMRI-derived radiomic features to determine the presence of axillary lymph node metastasis pre-operatively, yielding an accuracy of 84.43% (AUC of 0.919). Similarly, Dong et al. [45] achieved an AUC of 0.805 was achieved in their validation set.

Although these studies showed promising results, it is important to note that the evaluation of axillary adenopathy on MRI can be difficult as the axillary region may be incompletely included in the imaging FOV.

Breast Cancer Treatment Response Assessment and Prediction

NAC is the treatment of choice in patients with locally advanced breast cancer and in patients with early-stage triple negative breast cancer. MRI is the method of choice for NAC response assessment [46] and is superior to conventional imaging modalities (i.e., mammography, digital breast tomosynthesis, and ultrasound), which rely on changes in size or morphologic characteristics to evaluate tumor response with variable accuracy. Yet, the information regarding blood flow and vessel permeability provided by DCE MRI might

be less reliable in differentiating viable residual cancer form surrounding scar, necrosis, fibrosis, or treatment-related inflammation [47].

A growing number of studies have documented the ability of DWI to assess for early response to NAC, attributed to changes in water diffusivity, tumor cellularity, and cell membrane integrity within the tumor microenvironment related to cell lysis, necrosis, and the cytotoxic effect of the chemotherapy. For example, studies have reported that changes in ADC before and after the first chemotherapy administration can differentiate responders from non-responders [48–51]. A prospective study by Pereira et al. [52] involving 62 patients treated with NAC showed that patients who achieved pathologic complete response (pCR) (i.e., responders) had a higher increase in ADC between the first and second MRI (after 1 cycle of treatment) than non-responders and that these changes preceded changes in tumor dimensions. In the ACRIN 6698 multicenter trial [53] involving 272 women with breast cancer from 10 institutions treated with NAC, each woman underwent DWI before treatment, at 3 weeks (after 1 cycle of NAC), at 12 weeks, and after treatment. The percentage change in tumor ADC from before treatment (ΔADC) was measured at each time point. The authors concluded that ΔADC at 12 weeks was a significant independent predictor of pCR, with greater increase in tumor ADC corresponding to higher likelihood of pCR, and results further showed that the predictive value of ΔADC was highest in HR+/HER2− tumors (AUC = 0.76; 95% CI: 0.62–0.89; $p < .001$) (Fig. 3). Another study [51] concluded that there was no significant difference in pre-treatment ADC values between responders and non-responders generally, but when tumors were separated into subgroups, the authors were able to predict pCR using a cutoff ADC value of 0.995×10^{-3} mm^2/s for triple negative cancers and 0.971×10^{-3} mm^2/s, for HER2+ cancers. A meta-analysis [54] of 20 studies comprising 1490 patients demonstrated a pooled sensitivity of DWI of 89% (95% CI: 0.86–0.91), a specificity of 72%, and an AUC of 0.91 for predicting pCR.

Other studies have assessed response to NAC based solely on ADC values extrapolated from pre-treatment MRI. A meta-analysis by Surov et al. [55] comprising 1827 patients with different breast cancer subtypes showed that the pooled calculated pre-treatment mean ADC value was not significantly different between responders and non-responders and overlapped significantly.

Regarding the evaluation of axillary response to NAC, which is challenging using MRI, Grana-Lopez et al. [56] showed that changes in breast tumor ADC values were associated with axillary pCR. Nevertheless, the difference was not significant ($p = .058$), probably due to the small sample size. In that study, axillary pCR also showed correlations with ER negativity, HER2 positivity, and response of primary tumor. Meanwhile, Belli et al. [57] did not see significant differences in ADC before and after treatment in either responder or non-responders.

Recently, radiomics and AI applied to DWI or mpMRI combining DCE MRI and DWI have also been investigated for the prediction of treatment response. Choi et al. [58] developed a convolutional neural network model to predict response to NAC using PET/CT and DWI. The AUC for PET/CT was 0.89 when using pre-treatment images and 0.98 when using post-treatment images. The AUC for DWI was 0.70 and 0.53 when using pre- and post-treatment

images, respectively. Meanwhile, Tahmassebi et al. [59] showed that machine learning with mpMRI predicted pCR with an AUC of 0.86 after only two cycles of NAC, as well as predicted survival outcomes with high accuracy. Mani et al. [60] investigated the potential of mpMRI for the early prediction of response after just one cycle of NAC. In that study, imaging variables (DCE MRI, DWI), clinical data, and histopathologic variables were used for predictive modeling using machine learning. The AI model combining both imaging and clinical variables yielded the highest diagnostic accuracy of 0.90 with an AUC of 0.96. The same group conducted a follow-up study in 28 patients [61], incorporating a larger number of DCE MRI and DWI features (118 vs 13). Model accuracies were 82% alone and 86% when clinical and imaging features were combined, yielding a sensitivity of 88% and a specificity of 82%, respectively, outperforming the currently used RECIST approach that yielded an accuracy of 71%, sensitivity of 82%, and specificity of 65%. Elsewhere, the pre-treatment radiomics model by Liu et al. for predicting pCR in response to primary systemic treatment using both mpMRI and clinical information yielded an AUC of 0.86 [62].

Emerging Clinical Applications

Breast Cancer Screening

Several retrospective studies have attempted to investigate DWI for breast cancer screening in the real world [14, 63–79], where readers assigned a category based on binary classification or assigned a suspicion score on a scale similar to that of BI-RADS categories. Some of these studies included only intermediate-to-high risk patients who were asymptomatic [72, 74, 79], while others included patients with known malignancy [63–66]. DWI showed a mean sensitivity of 81% (range, 44–97%) and a mean specificity of 88% (range 73–96%) across studies overall, but studies that more closely approximated screening settings (included negative or benign cases) reported a mean sensitivity of 76% (range, 45–100%) [64, 72, 74, 76–79].

DWI can result in false-negative findings for certain types of breast cancer (e.g., DCIS, mucinous carcinoma, small cancers, and invasive lobular cancer, due to their imaging characteristics and the low spatial resolution of conventional DWI) [14, 64, 65, 67, 69, 74, 76–78]. DWI can also produce false positives [73, 74, 77, 78, 80]. For example, complicated or proteinaceous cysts are known to exhibit restricted diffusion [77]. Fibroadenomas may also be mistaken as a suspicious finding due to their wide range of possible ADC values [81]. Finally, false positives can be produced by artifactual signal such as occurs near the nipple-areolar complex, which is prone to susceptibility-based distortion on DWI [73, 74].

To help define the target population for DWI-based screening, the ongoing Diffusion-Weighted MRI Screening Trial (DWIST, NCT03835897) is comparing the screening performance of DWI against mammography, ultrasound, and DCE MRI in high-risk women [82]. Other trials are investigating the use of DWI for breast cancer screening in women with a personal history of breast cancer (NCT04619186) and in women with dense breast tissue (NCT03607552). One trial is investigating the use of DWI in screening the contralateral breast in women with newly diagnosed breast cancers (NCT04656639).

Practical Aspects for Clinical Implementation, Challenges, and Limitations

For all breast imaging modalities including DWI, uniform language is needed to describe findings, interpret results, and recommend treatment. Past studies have explored various strategies for interpreting DWI in breast cancer screening. Such studies typically focus on the initial identification of specific regions showing increased signal intensity on DWI, often considering factors like quantitative ADC evaluations, morphologic features, and appearances on other non-enhanced sequences such as T1- and T2-weighted images [64, 72–74, 76–79]. The DWIST group, in 2019, suggested a standardized set of terms and criteria for interpreting unenhanced MRI, including both DWI and pre-contrast T1- and T2-weighted images. Within these guidelines, an ADC threshold of 1.3×10^{-3} mm2/s was established, drawing upon a diffusion-based lexicon from EUSOBI, to improve positive predictive values.

Despite this progress, barriers limiting the widespread use of DWI remain, namely the variable image quality and the lack of technical standardization.

Standardization and Optimization

A major obstacle to the widespread clinical adoption of DWI is the significant variation in acquisition methods across different research studies and healthcare facilities, leading to inconsistencies in image quality. Additionally, divergent approaches to data analysis, such as post-processing techniques, the selection of b-values for ADC calculations, and methods for defining ROI create discrepancies in ADC values even for similar breast pathologies. This lack of standardization hampers the development of universally applicable interpretation guidelines for breast DWI and undermines the reliable assessment of its clinical usefulness.

Aiming for standardization as well as improved image quality, the EUSOBI International Breast DWI working group proposed a set of consensus guidelines for clinical breast DWI. Among the fundamental acquisition prerequisites recommended are: the employment of a spin-echo prepared echo-planar imaging (EPI) pulse sequence, axial image capture with an in-plane spatial resolution of 2×2 mm^2 or less and a slice thickness of 4 mm or less, a parallel imaging acceleration factor of 2 or higher, a TR of at least 3 seconds coupled with the shortest feasible TE, and a minimum of two b-values (specifically, 0 and 800 s/mm^2). They emphasized the importance of high-quality shimming and fat suppression as well as the use of higher field strength scanners (3 T vs 1.5 T) along with high-performance gradients and breast coils with a greater number of channels to maximize overall image quality. For quantitative ADC analysis, a maximum b-value of 800 s/mm^2 is recommended [83].

A variety of ROI methods have been used, ranging from the hot-spot method (identification of the subregion exhibiting the lowest ADC) to 3D multislice whole-tumor measurement. Several studies support the hotspot method, showing that it yields a similar diagnostic performance to whole-lesion measurement for classifying suspicious breast lesions and may be easier to perform in clinical environments with limited ROI software tools [84–86]. Besides EUSOBI, the Radiological Society of North America Quantitative Imaging Biomarkers Alliance has released DWI acquisition and analysis specifications to support

the reliable use of ADC as a quantitative marker of neoadjuvant treatment response (with defined CIs) [87].

For screening applications, evidence supports the use of high b-value (1200–1500 s/mm^2) images to maximize the visibility of malignant lesions [4, 88, 89]. Computed DWI is a convenient technique whereby high b-value (b ≥ 1000 s/mm^2) images are synthesized from images acquired at a lower b-values [75, 90, 91] (Fig. 4).

Technical Challenges

Several acquisition factors can directly affect breast DWI image quality and reliability. Choice of magnetic field strength can significantly impact various aspects of diffusion imaging. Higher field strength is generally preferable for breast DWI, as it increases the SNR, thus improving image quality and facilitating higher spatial resolution. However, field inhomogeneity effects can also be exacerbated at higher field strengths, necessitating more advanced shimming approaches to avoid detrimental artifacts and susceptibility-based distortions. Importantly, ADC is not directly influenced by field strength, and a study has found no significant differences in sensitivity or specificity for breast cancer diagnosis with respect to clinical field strength (20).

In addition to field strength, ensuring high-quality DWI requires addressing artifacts arising from factors like patient motion, inadequate shimming and fat suppression, and eddy currents. Although some artifacts may be avoided during image acquisition or corrected through post-processing techniques [83, 92], comprehensive and effective management of these factors is crucial to minimize the frequency of unsuccessful examinations. Two prospective multicenter trials of breast DWI, each incorporating a variety of scanner platforms and field strengths, reported that 13–25% of examinations were excluded on centralized review due to insufficient image quality for quantitative lesion ADC analysis [9, 93], citing issues of excessive artifacts, fat suppression failure, and poor SNR [93]. Reported rates of unsuccessful examinations vary widely in the literature, with technical failure rates of 7.5–17.5% reported across five independent single-center studies evaluating ADC measures in DCE MRI-detected lesions [10]. Much lower technical failure rates have been reported in some studies of breast DWI using more rigorous acquisition approaches to maximize image quality (e.g., technical failure rates of 1% and 3% in two large DWI screening studies incorporating 3-T field strength and advanced multi-shot EPI acquisitions [64, 72]), suggesting the potential of technical advancements to improve overall image quality and reliability of DWI.

Emerging Techniques

The quality issues with DWI are largely due to the technique’s dependence on single-shot EPI sequences. Specific challenges in breast imaging include the need for a large FOV for bilateral coverage, off-center imaging, and air-tissue interfaces that worsen field inhomogeneities and distortions. Moreover, the significant fat content in breast tissue necessitates suppression techniques to prevent chemical shift artifacts. Consequently, traditional breast DWI is often impeded by lower spatial resolution and is susceptible to artifacts and distortions caused by magnetic susceptibility.

New acquisition methods that span different vendor platforms aim to overcome these limitations. Multi-shot approaches like readout-segmented and multiplexed sensitivity-encoding reduce the required matrix sizes and associated readout times per excitation, thus improving resolution [94] (Fig. 5). Reduced FOV EPI also contributes to this aim [4, 95]. Although these approaches lead to enhanced spatial resolution and fewer artifacts, they often result in longer scan times or reduced coverage. Simultaneous multi-slice imaging methods support higher resolution by speeding up acquisitions in the slice dimension, allowing for a greater number of thinner slices without compromising coverage or scan time [96, 97]. Additionally, AI-based reconstruction methods for image denoising are gaining traction among scanner manufacturers [98] (Fig. 6). In combination with other DWI post-processing techniques, these methods can improve image quality by reducing magnetic field inhomogeneity-related EPI distortions and artifacts resulting from eddy currents and motion, as well as by correcting b-value inaccuracies resulting from gradient non-linearities [4].

Conclusion

Breast DWI has been used for a variety of imaging applications in breast cancer imaging, with the current main applications being the differentiation of benign and malignant enhancing lesions, treatment response assessment, and prediction of response to chemotherapy for patient undergoing NAC. Emerging applications of breast DWI include breast cancer detection, lesion characterization, and AI-enhanced DWI to improve lesion characterization and the prediction and evaluation of treatment response. The use of DWI for non-contrast screening remains an active area of research, with ongoing prospective multi-center trials, which will likely increase in number given the current technical advances that seek to improve image quality and lesion conspicuity. Along with techniques to improve image quality, standardized acquisition protocols and post-processing methods are also needed. Specifically, quantitative assessment of DWI with ADC mapping may help increase specificity of DCE MRI; however, standardized acquisition protocols, ADC calculation methods, and ROI measurement methods are currently lacking, resulting in considerable differences in the reported ADC values of similar breast pathologies. In all, emerging technical advances and efforts in standardization to overcome the current limitations of DWI might prove valuable to improve the day-to-day clinical use of breast DWI.

Funding sources:

This study was supported in part through the NIH/NCI Cancer Center Support Grants P30 CA008748 and P30 CA015704, and R01 CA207290.

Author disclosures:

Katja Pinker declares being part of speakers bureaus for the European Society of Breast Imaging (active), Bayer (ended), Siemens Healthineers (ended), DKD 2019 (ended), Olea Medical (ended), and Roche (ended); consulting for Genentech, Merantix Healthcare, AURA Health Technologies. Guerbet, and Bayer. Savannah Partridge declares receiving consultant fees from Guerbet (ended) and research support paid to her institution from GE Healthcare (grant) and Philips Healthcare (in-kind support). The remaining authors declare no competing interests.

References

1. Mann RM, Cho N, Moy L. Breast MRI: State of the Art. Radiology 2019; 292:520–536 [PubMed: 31361209]

2. Leithner D, Wengert GJ, Helbich TH, Thakur S, Ochoa-Albiztegui RE, Morris EA, Pinker K. Clinical role of breast MRI now and going forward. Clin Radiol 2018; 73:700–714 [PubMed: 29229179]

3. Lo Gullo R, Sevilimedu V, Baltzer P, et al. A survey by the European Society of Breast Imaging on the implementation of breast diffusion-weighted imaging in clinical practice. Eur Radiol 2022; 32:6588–6597 [PubMed: 35507050]

4. Amornsiripanitch N, Bickelhaupt S, Shin HJ, Dang M, Rahbar H, Pinker K, Partridge SC. Diffusion-weighted MRI for Unenhanced Breast Cancer Screening. Radiology 2019; 293:504–520 [PubMed: 31592734]

5. Yoshikawa MI, Ohsumi S, Sugata S, et al. Relation between cancer cellularity and apparent diffusion coefficient values using diffusion-weighted magnetic resonance imaging in breast cancer. Radiat Med 2008; 26:222–226 [PubMed: 18509722]

6. Jiang R, Ma Z, Dong H, Sun S, Zeng X, Li X. Diffusion tensor imaging of breast lesions: evaluation of apparent diffusion coefficient and fractional anisotropy and tissue cellularity. Br J Radiol 2016; 89:20160076 [PubMed: 27302492]

7. Chen L, Liu M, Bao J, et al. The correlation between apparent diffusion coefficient and tumor cellularity in patients: a meta-analysis. PLoS One 2013; 8:e79008 [PubMed: 24244402]

8. Zhang L, Tang M, Min Z, Lu J, Lei X, Zhang X. Accuracy of combined dynamic contrast-enhanced magnetic resonance imaging and diffusion-weighted imaging for breast cancer detection: a meta-analysis. Acta Radiol 2016; 57:651–660 [PubMed: 26275624]

9. Rahbar H, Zhang Z, Chenevert TL, et al. Utility of Diffusion-weighted Imaging to Decrease Unnecessary Biopsies Prompted by Breast MRI: A Trial of the ECOG-ACRIN Cancer Research Group (A6702). Clin Cancer Res 2019; 25:1756–1765 [PubMed: 30647080]

10. Clauser P, Krug B, Bickel H, et al. Diffusion-weighted Imaging Allows for Downgrading MR BI-RADS 4 Lesions in Contrast-enhanced MRI of the Breast to Avoid Unnecessary Biopsy. Clin Cancer Res 2021; 27:1941–1948 [PubMed: 33446565]

11. Surov A, Meyer HJ, Wienke A. Can apparent diffusion coefficient (ADC) distinguish breast cancer from benign breast findings? A meta-analysis based on 13 847 lesions. BMC Cancer 2019; 19:955 [PubMed: 31615463]

12. Shi RY, Yao QY, Wu LM, Xu JR. Breast Lesions: Diagnosis Using Diffusion Weighted Imaging at 1.5T and 3.0T-Systematic Review and Meta-analysis. Clin Breast Cancer 2018; 18:e305–e320 [PubMed: 28802529]

13. Dorrius MD, Dijkstra H, Oudkerk M, Sijens PE. Effect of b value and pre-admission of contrast on diagnostic accuracy of 1.5-T breast DWI: a systematic review and meta-analysis. Eur Radiol 2014; 24:2835–2847 [PubMed: 25103535]

14. Pinker K, Moy L, Sutton EJ, et al. Diffusion-Weighted Imaging With Apparent Diffusion Coefficient Mapping for Breast Cancer Detection as a Stand-Alone Parameter: Comparison With Dynamic Contrast-Enhanced and Multiparametric Magnetic Resonance Imaging. Invest Radiol 2018; 53:587–595 [PubMed: 29620604]

15. Li Y, Chen J, Yang Z, et al. Contrasts Between Diffusion-Weighted Imaging and Dynamic Contrast-Enhanced MR in Diagnosing Malignancies of Breast Nonmass Enhancement Lesions Based on Morphologic Assessment. J Magn Reson Imaging 2023;

16. Avendano D, Marino MA, Leithner D, et al. Limited role of DWI with apparent diffusion coefficient mapping in breast lesions presenting as non-mass enhancement on dynamic contrast-enhanced MRI. Breast Cancer Res 2019; 21:136 [PubMed: 31801635]

17. Marino MA, Avendano D, Sevilimedu V, et al. Limited value of multiparametric MRI with dynamic contrast-enhanced and diffusion-weighted imaging in non-mass enhancing breast tumors. Eur J Radiol 2022; 156:110523 [PubMed: 36122521]

18. Dalmis MU, Gubern-Merida A, Vreemann S, Bult P, Karssemeijer N, Mann R, Teuwen J. Artificial Intelligence-Based Classification of Breast Lesions Imaged With a Multiparametric Breast MRI Protocol With Ultrafast DCE-MRI, T2, and DWI. Invest Radiol 2019; 54:325–332 [PubMed: 30652985]

19. Feng H, Cao J, Wang H, Xie Y, Yang D, Feng J, Chen B. A knowledge-driven feature learning and integration method for breast cancer diagnosis on multi-sequence MRI. Magn Reson Imaging 2020; 69:40–48 [PubMed: 32173583]
20. Horvat JV, Bernard-Davila B, Helbich TH, et al. Diffusion-weighted imaging (DWI) with apparent diffusion coefficient (ADC) mapping as a quantitative imaging biomarker for prediction of immunohistochemical receptor status, proliferation rate, and molecular subtypes of breast cancer. J Magn Reson Imaging 2019; 50:836–846 [PubMed: 30811717]
21. Leithner D, Bernard-Davila B, Martinez DF, et al. Radiomic Signatures Derived from Diffusion-Weighted Imaging for the Assessment of Breast Cancer Receptor Status and Molecular Subtypes. Mol Imaging Biol 2020; 22:453–461 [PubMed: 31209778]
22. Teng X, Zhang J, Zhang X, et al. Noninvasive imaging signatures of HER2 and HR using ADC in invasive breast cancer: repeatability, reproducibility, and association with pathological complete response to neoadjuvant chemotherapy. Breast Cancer Res 2023; 25:77 [PubMed: 37381020]
23. Andreassen MMS, Loubrie S, Tong MW, et al. Restriction spectrum imaging with elastic image registration for automated evaluation of response to neoadjuvant therapy in breast cancer. Front Oncol 2023; 13:1237720 [PubMed: 37781199]
24. Bickel H, Pinker-Domenig K, Bogner W, et al. Quantitative apparent diffusion coefficient as a noninvasive imaging biomarker for the differentiation of invasive breast cancer and ductal carcinoma in situ. Invest Radiol 2015; 50:95–100 [PubMed: 25333308]
25. Hussein H, Chung C, Moshonov H, Miller N, Kulkarni SR, Scaranelo AM. Evaluation of Apparent Diffusion Coefficient to Predict Grade, Microinvasion, and Invasion in Ductal Carcinoma In Situ of the Breast. Acad Radiol 2015; 22:1483–1488 [PubMed: 26391856]
26. Mori N, Ota H, Mugikura S, et al. Detection of invasive components in cases of breast ductal carcinoma in situ on biopsy by using apparent diffusion coefficient MR parameters. Eur Radiol 2013; 23:2705–2712 [PubMed: 23732688]
27. Rahbar H, Partridge SC, Eby PR, Demartini WB, Gutierrez RL, Peacock S, Lehman CD. Characterization of ductal carcinoma in situ on diffusion weighted breast MRI. Eur Radiol 2011; 21:2011–2019 [PubMed: 21562806]
28. Costantini M, Belli P, Rinaldi P, et al. Diffusion-weighted imaging in breast cancer: relationship between apparent diffusion coefficient and tumour aggressiveness. Clin Radiol 2010; 65:1005–1012 [PubMed: 21070905]
29. Choi SY, Chang YW, Park HJ, Kim HJ, Hong SS, Seo DY. Correlation of the apparent diffusion coefficiency values on diffusion-weighted imaging with prognostic factors for breast cancer. Br J Radiol 2012; 85:e474–479 [PubMed: 22128125]
30. Guvenc I, Akay S, Ince S, Yildiz R, Kilbas Z, Oysul FG, Tasar M. Apparent diffusion coefficient value in invasive ductal carcinoma at 3.0 Tesla: is it correlated with prognostic factors? Br J Radiol 2016; 89:20150614 [PubMed: 26853508]
31. Jeh SK, Kim SH, Kim HS, Kang BJ, Jeong SH, Yim HW, Song BJ. Correlation of the apparent diffusion coefficient value and dynamic magnetic resonance imaging findings with prognostic factors in invasive ductal carcinoma. J Magn Reson Imaging 2011; 33:102–109 [PubMed: 21182127]
32. Kamitani T, Matsuo Y, Yabuuchi H, et al. Correlations between apparent diffusion coefficient values and prognostic factors of breast cancer. Magn Reson Med Sci 2013; 12:193–199 [PubMed: 23857151]
33. Kim SH, Cha ES, Kim HS, et al. Diffusion-weighted imaging of breast cancer: correlation of the apparent diffusion coefficient value with prognostic factors. J Magn Reson Imaging 2009; 30:615–620 [PubMed: 19711411]
34. Martincich L, Deantoni V, Bertotto I, et al. Correlations between diffusion-weighted imaging and breast cancer biomarkers. Eur Radiol 2012; 22:1519–1528 [PubMed: 22411304]
35. Kim JY, Seo HB, Park S, et al. Early-stage invasive ductal carcinoma: Association of tumor apparent diffusion coefficient values with axillary lymph node metastasis. Eur J Radiol 2015; 84:2137–2143 [PubMed: 26318821]

36. Leithner D, Mayerhoefer ME, Martinez DF, Jochelson MS, Morris EA, Thakur SB, Pinker K. Non-Invasive Assessment of Breast Cancer Molecular Subtypes with Multiparametric Magnetic Resonance Imaging Radiomics. J Clin Med 2020; 9
37. Huang Y, Wei L, Hu Y, et al. Multi-Parametric MRI-Based Radiomics Models for Predicting Molecular Subtype and Androgen Receptor Expression in Breast Cancer. Front Oncol 2021; 11:706733 [PubMed: 34490107]
38. Liu W, Cheng Y, Liu Z, et al. Preoperative Prediction of Ki-67 Status in Breast Cancer with Multiparametric MRI Using Transfer Learning. Acad Radiol 2021; 28:e44–e53 [PubMed: 32278690]
39. Zhang Y, Zhu Y, Zhang K, et al. Invasive ductal breast cancer: preoperative predict Ki-67 index based on radiomics of ADC maps. Radiol Med 2020; 125:109–116 [PubMed: 31696388]
40. Fan M, Yuan W, Zhao W, Xu M, Wang S, Gao X, Li L. Joint Prediction of Breast Cancer Histological Grade and Ki-67 Expression Level Based on DCE-MRI and DWI Radiomics. IEEE J Biomed Health Inform 2020; 24:1632–1642 [PubMed: 31794406]
41. Fan M, Liu Z, Xu M, Wang S, Zeng T, Gao X, Li L. Generative adversarial network-based super-resolution of diffusion-weighted imaging: Application to tumour radiomics in breast cancer. NMR Biomed 2020; 33:e4345 [PubMed: 32521567]
42. Guvenc I, Whitman GJ, Liu P, Yalniz C, Ma J, Dogan BE. Diffusion-weighted MR imaging increases diagnostic accuracy of breast MR imaging for predicting axillary metastases in breast cancer patients. Breast J 2019; 25:47–55 [PubMed: 30444286]
43. Fardanesh R, Thakur SB, Sevilimedu V, et al. Differentiation Between Benign and Metastatic Breast Lymph Nodes Using Apparent Diffusion Coefficients. Front Oncol 2022; 12:795265 [PubMed: 35280791]
44. Chai R, Ma H, Xu M, et al. Differentiating axillary lymph node metastasis in invasive breast cancer patients: A comparison of radiomic signatures from multiparametric breast MR sequences. J Magn Reson Imaging 2019; 50:1125–1132 [PubMed: 30848041]
45. Dong Y, Feng Q, Yang W, et al. Preoperative prediction of sentinel lymph node metastasis in breast cancer based on radiomics of T2-weighted fat-suppression and diffusion-weighted MRI. Eur Radiol 2018; 28:582–591 [PubMed: 28828635]
46. Dubsky P, Pinker K, Cardoso F, et al. Breast conservation and axillary management after primary systemic therapy in patients with early-stage breast cancer: the Lucerne toolbox. Lancet Oncol 2021; 22:e18–e28 [PubMed: 33387500]
47. Fujimoto H, Kazama T, Nagashima T, et al. Diffusion-weighted imaging reflects pathological therapeutic response and relapse in breast cancer. Breast cancer 2014; 21:724–731 [PubMed: 23400545]
48. Galban CJ, Ma B, Malyarenko D, et al. Multi-site clinical evaluation of DW-MRI as a treatment response metric for breast cancer patients undergoing neoadjuvant chemotherapy. PLoS One 2015; 10:e0122151 [PubMed: 25816249]
49. Richard R, Thomassin I, Chapellier M, et al. Diffusion-weighted MRI in pretreatment prediction of response to neoadjuvant chemotherapy in patients with breast cancer. Eur Radiol 2013; 23:2420–2431 [PubMed: 23652844]
50. Liu S, Ren R, Chen Z, Wang Y, Fan T, Li C, Zhang P. Diffusion-weighted imaging in assessing pathological response of tumor in breast cancer subtype to neoadjuvant chemotherapy. J Magn Reson Imaging 2015; 42:779–787 [PubMed: 25580585]
51. Bufi E, Belli P, Costantini M, et al. Role of the Apparent Diffusion Coefficient in the Prediction of Response to Neoadjuvant Chemotherapy in Patients With Locally Advanced Breast Cancer. Clin Breast Cancer 2015; 15:370–380 [PubMed: 25891905]
52. Pereira NP, Curi C, Osorio C, Marques EF, Makdissi FB, Pinker K, Bitencourt AGV. Diffusion-Weighted Magnetic Resonance Imaging of Patients with Breast Cancer Following Neoadjuvant Chemotherapy Provides Early Prediction of Pathological Response - A Prospective Study. Sci Rep 2019; 9:16372 [PubMed: 31705004]
53. Partridge SC, Zhang Z, Newitt DC, et al. Diffusion-weighted MRI Findings Predict Pathologic Response in Neoadjuvant Treatment of Breast Cancer: The ACRIN 6698 Multicenter Trial. Radiology 2018; 289:618–627 [PubMed: 30179110]

54. Gao W, Guo N, Dong T. Diffusion-weighted imaging in monitoring the pathological response to neoadjuvant chemotherapy in patients with breast cancer: a meta-analysis. World J Surg Oncol 2018; 16:145 [PubMed: 30021656]
55. Surov A, Wienke A, Meyer HJ. Pretreatment apparent diffusion coefficient does not predict therapy response to neoadjuvant chemotherapy in breast cancer. Breast 2020; 53:59–67 [PubMed: 32652460]
56. Graña-López L, Pérez-Ramos T, Maciñeira FA, Villares Á, Vázquez-Caruncho M. Predicting axillary response to neoadjuvant chemotherapy: the role of diffusion weighted imaging. Br J Radiol 2022; 95:20210511 [PubMed: 34757835]
57. Belli P, Bufi E, Buccheri C, et al. Role of DWI assessing nodal involvement and response to neoadjuvant chemotherapy in advanced breast cancer. Eur Rev Med Pharmacol Sci 2017; 21:695–705 [PubMed: 28272714]
58. Choi JH, Kim HA, Kim W, et al. Early prediction of neoadjuvant chemotherapy response for advanced breast cancer using PET/MRI image deep learning. Sci Rep 2020; 10:21149 [PubMed: 33273490]
59. Tahmassebi A, Wengert GJ, Helbich TH, et al. Impact of Machine Learning With Multiparametric Magnetic Resonance Imaging of the Breast for Early Prediction of Response to Neoadjuvant Chemotherapy and Survival Outcomes in Breast Cancer Patients. Invest Radiol 2019; 54:110–117 [PubMed: 30358693]
60. Mani S, Chen Y, Arlinghaus LR, et al. Early prediction of the response of breast tumors to neoadjuvant chemotherapy using quantitative MRI and machine learning. AMIA Annu Symp Proc 2011; 2011:868–877 [PubMed: 22195145]
61. Mani S, Chen Y, Li X, et al. Machine learning for predicting the response of breast cancer to neoadjuvant chemotherapy. J Am Med Inform Assoc 2013; 20:688–695 [PubMed: 23616206]
62. Liu Z, Li Z, Qu J, et al. Radiomics of Multiparametric MRI for Pretreatment Prediction of Pathologic Complete Response to Neoadjuvant Chemotherapy in Breast Cancer: A Multicenter Study. Clin Cancer Res 2019; 25:3538–3547 [PubMed: 30842125]
63. Shin HJ, Chae EY, Choi WJ, et al. Diagnostic Performance of Fused Diffusion-Weighted Imaging Using Unenhanced or Postcontrast T1-Weighted MR Imaging in Patients With Breast Cancer. Medicine (Baltimore) 2016; 95:e3502 [PubMed: 27124054]
64. Ha SM, Chang JM, Lee SH, Kim ES, Kim SY, Cho N, Moon WK. Diffusion-weighted MRI at 3.0 T for detection of occult disease in the contralateral breast in women with newly diagnosed breast cancer. Breast Cancer Res Treat 2020; 182:283–297 [PubMed: 32447596]
65. Kuroki-Suzuki S, Kuroki Y, Nasu K, Nawano S, Moriyama N, Okazaki M. Detecting breast cancer with non-contrast MR imaging: combining diffusion-weighted and STIR imaging. Magn Reson Med Sci 2007; 6:21–27 [PubMed: 17510539]
66. Yoshikawa MI, Ohsumi S, Sugata S, Kataoka M, Takashima S, Kikuchi K, Mochizuki T. Comparison of breast cancer detection by diffusion-weighted magnetic resonance imaging and mammography. Radiat Med 2007; 25:218–223 [PubMed: 17581710]
67. Baltzer PA, Benndorf M, Dietzel M, Gajda M, Camara O, Kaiser WA. Sensitivity and specificity of unenhanced MR mammography (DWI combined with T2-weighted TSE imaging, ueMRM) for the differentiation of mass lesions. Eur Radiol 2010; 20:1101–1110 [PubMed: 19936758]
68. Wu LM, Chen J, Hu J, Gu HY, Xu JR, Hua J. Diffusion-weighted magnetic resonance imaging combined with T2-weighted images in the detection of small breast cancer: a single-center multi-observer study. Acta Radiol 2014; 55:24–31 [PubMed: 23878358]
69. Bickelhaupt S, Laun FB, Tesdorff J, et al. Fast and Noninvasive Characterization of Suspicious Lesions Detected at Breast Cancer X-Ray Screening: Capability of Diffusion-weighted MR Imaging with MIPs. Radiology 2016; 278:689–697 [PubMed: 26418516]
70. Baltzer PAT, Bickel H, Spick C, et al. Potential of Noncontrast Magnetic Resonance Imaging With Diffusion-Weighted Imaging in Characterization of Breast Lesions: Intraindividual Comparison With Dynamic Contrast-Enhanced Magnetic Resonance Imaging. Invest Radiol 2018; 53:229–235 [PubMed: 29190227]

71. Bu Y, Xia J, Joseph B, et al. Non-contrast MRI for breast screening: preliminary study on detectability of benign and malignant lesions in women with dense breasts. Breast Cancer Res Treat 2019; 177:629–639 [PubMed: 31325074]
72. Kang JW, Shin HJ, Shin KC, Chae EY, Choi WJ, Cha JH, Kim HH. Unenhanced magnetic resonance screening using fused diffusion-weighted imaging and maximum-intensity projection in patients with a personal history of breast cancer: role of fused DWI for postoperative screening. Breast Cancer Res Treat 2017; 165:119–128 [PubMed: 28577079]
73. Kazama T, Kuroki Y, Kikuchi M, et al. Diffusion-weighted MRI as an adjunct to mammography in women under 50 years of age: an initial study. J Magn Reson Imaging 2012; 36:139–144 [PubMed: 22359367]
74. McDonald ES, Hammersley JA, Chou SH, et al. Performance of DWI as a Rapid Unenhanced Technique for Detecting Mammographically Occult Breast Cancer in Elevated-Risk Women With Dense Breasts. AJR Am J Roentgenol 2016; 207:205–216 [PubMed: 27077731]
75. O'Flynn EA, Blackledge M, Collins D, et al. Evaluating the diagnostic sensitivity of computed diffusion-weighted MR imaging in the detection of breast cancer. J Magn Reson Imaging 2016; 44:130–137 [PubMed: 26762608]
76. Rotili A, Trimboli RM, Penco S, Pesapane F, Tantrige P, Cassano E, Sardanelli F. Double reading of diffusion-weighted magnetic resonance imaging for breast cancer detection. Breast Cancer Res Treat 2020; 180:111–120 [PubMed: 31938940]
77. Telegrafo M, Rella L, Stabile Ianora AA, Angelelli G, Moschetta M. Unenhanced breast MRI (STIR, T2-weighted TSE, DWIBS): An accurate and alternative strategy for detecting and differentiating breast lesions. Magn Reson Imaging 2015; 33:951–955 [PubMed: 26117691]
78. Trimboli RM, Verardi N, Cartia F, Carbonaro LA, Sardanelli F. Breast cancer detection using double reading of unenhanced MRI including T1-weighted, T2-weighted STIR, and diffusion-weighted imaging: a proof of concept study. AJR Am J Roentgenol 2014; 203:674–681 [PubMed: 25148175]
79. Yabuuchi H, Matsuo Y, Sunami S, et al. Detection of non-palpable breast cancer in asymptomatic women by using unenhanced diffusion-weighted and T2-weighted MR imaging: comparison with mammography and dynamic contrast-enhanced MR imaging. Eur Radiol 2011; 21:11–17 [PubMed: 20640898]
80. Belli P, Bufi E, Bonatesta A, et al. Unenhanced breast magnetic resonance imaging: detection of breast cancer. Eur Rev Med Pharmacol Sci 2016; 20:4220–4229 [PubMed: 27831654]
81. Parsian S, Rahbar H, Allison KH, Demartini WB, Olson ML, Lehman CD, Partridge SC. Nonmalignant breast lesions: ADCs of benign and high-risk subtypes assessed as false-positive at dynamic enhanced MR imaging. Radiology 2012; 265:696–706 [PubMed: 23033500]
82. Shin HJ, Lee SH, Park VY, et al. Diffusion-Weighted Magnetic Resonance Imaging for Breast Cancer Screening in High-Risk Women: Design and Imaging Protocol of a Prospective Multicenter Study in Korea. J Breast Cancer 2021; 24:218–228 [PubMed: 33913277]
83. Baltzer P, Mann RM, Iima M, et al. Diffusion-weighted imaging of the breast-a consensus and mission statement from the EUSOBI International Breast Diffusion-Weighted Imaging working group. Eur Radiol 2020; 30:1436–1450 [PubMed: 31786616]
84. McDonald ES, Romanoff J, Rahbar H, et al. Mean Apparent Diffusion Coefficient Is a Sufficient Conventional Diffusion-weighted MRI Metric to Improve Breast MRI Diagnostic Performance: Results from the ECOG-ACRIN Cancer Research Group A6702 Diffusion Imaging Trial. Radiology 2021; 298:60–70 [PubMed: 33201788]
85. Bickel H, Pinker K, Polanec S, et al. Diffusion-weighted imaging of breast lesions: Region-of-interest placement and different ADC parameters influence apparent diffusion coefficient values. Eur Radiol 2017; 27:1883–1892 [PubMed: 27578047]
86. Arponent O, Sudah M, Masarwah A, et al. Diffusion-Weighted Imaging in 3.0 Tesla Breast MRI: Diagnostic Performance and Tumor Characterization Using Small Subregions vs. Whole Tumor Regions of Interest. PLOS ONE 2015; 10:e0138702 [PubMed: 26458106]
87. RSNA Quantiative Imaging Biomarkers Alliance. QIBA Profile: Diffusion-Weighted Magnetic Resonance Imaging (DWI). https://qibawiki.rsna.org/index.php/Profiles.

88. DelPriore MR, Biswas D, Hippe DS, et al. Breast Cancer Conspicuity on Computed Versus Acquired High b-Value Diffusion-Weighted MRI. Acad Radiol 2020;
89. Woodhams R, Inoue Y, Ramadan S, Hata H, Ozaki M. Diffusion-weighted imaging of the breast: comparison of b-values 1000 s/mm(2) and 1500 s/mm(2). Magn Reson Med Sci 2013; 12:229–234 [PubMed: 23857152]
90. DelPriore MR, Biswas D, Hippe DS, et al. Breast Cancer Conspicuity on Computed Versus Acquired High b-Value Diffusion-Weighted MRI. Acad Radiol 2021; 28:1108–1117 [PubMed: 32307271]
91. Bickel H, Polanec SH, Wengert G, Pinker K, Bogner W, Helbich TH, Baltzer PA. Diffusion-Weighted MRI of Breast Cancer: Improved Lesion Visibility and Image Quality Using Synthetic b-Values. J Magn Reson Imaging 2019; 50:1754–1761 [PubMed: 31136044]
92. Baltzer P, Mann RM, Iima M, et al. Diffusion-weighted imaging of the breast-a consensus and mission statement from the EUSOBI International Breast Diffusion-Weighted Imaging working group. Eur Radiol 2020; 30:1436–1450 [PubMed: 31786616]
93. Newitt DC, Zhang Z, Gibbs JE, et al. Test-retest repeatability and reproducibility of ADC measures by breast DWI: Results from the ACRIN 6698 trial. J Magn Reson Imaging 2019; 49:1617–1628 [PubMed: 30350329]
94. Naranjo ID, Gullo RL, Morris EA, et al. High-Spatial-Resolution Multishot Multiplexed Sensitivity-encoding Diffusion-weighted Imaging for Improved Quality of Breast Images and Differentiation of Breast Lesions: A Feasibility Study. Radiology: Imaging Cancer 2020; 2
95. Partridge SC, Nissan N, Rahbar H, Kitsch AE, Sigmund EE. Diffusion-weighted breast MRI: Clinical applications and emerging techniques. J Magn Reson Imaging 2017; 45:337–355 [PubMed: 27690173]
96. Filli L, Ghafoor S, Kenkel D, et al. Simultaneous multi-slice readout-segmented echo planar imaging for accelerated diffusion-weighted imaging of the breast. Eur J Radiol 2016; 85:274–278 [PubMed: 26547123]
97. Biswas D, Hippe DS, Wang Y, et al. Accelerated Breast Diffusion-weighted Imaging Using Multiband Sensitivity Encoding with the CAIPIRINHA Method: Clinical Experience at 3 T. Radiol Imaging Cancer 2022; 4:e210063 [PubMed: 35029517]
98. Lin DJ, Johnson PM, Knoll F, Lui YW. Artificial Intelligence for MR Image Reconstruction: An Overview for Clinicians. J Magn Reson Imaging 2021; 53:1015–1028 [PubMed: 32048372]

Highlights

- DWI is a fast noncontrast imaging technique that may supplement and overcome the challenges of DCE MRI in breast cancer imaging.
- Current applications of DWI include breast cancer detection and characterization, prognostication, and neoadjuvant chemotherapy response prediction. DWI is also being investigated for breast cancer screening.
- Historic image quality issues when performing DWI are being addressed through several technical advances.

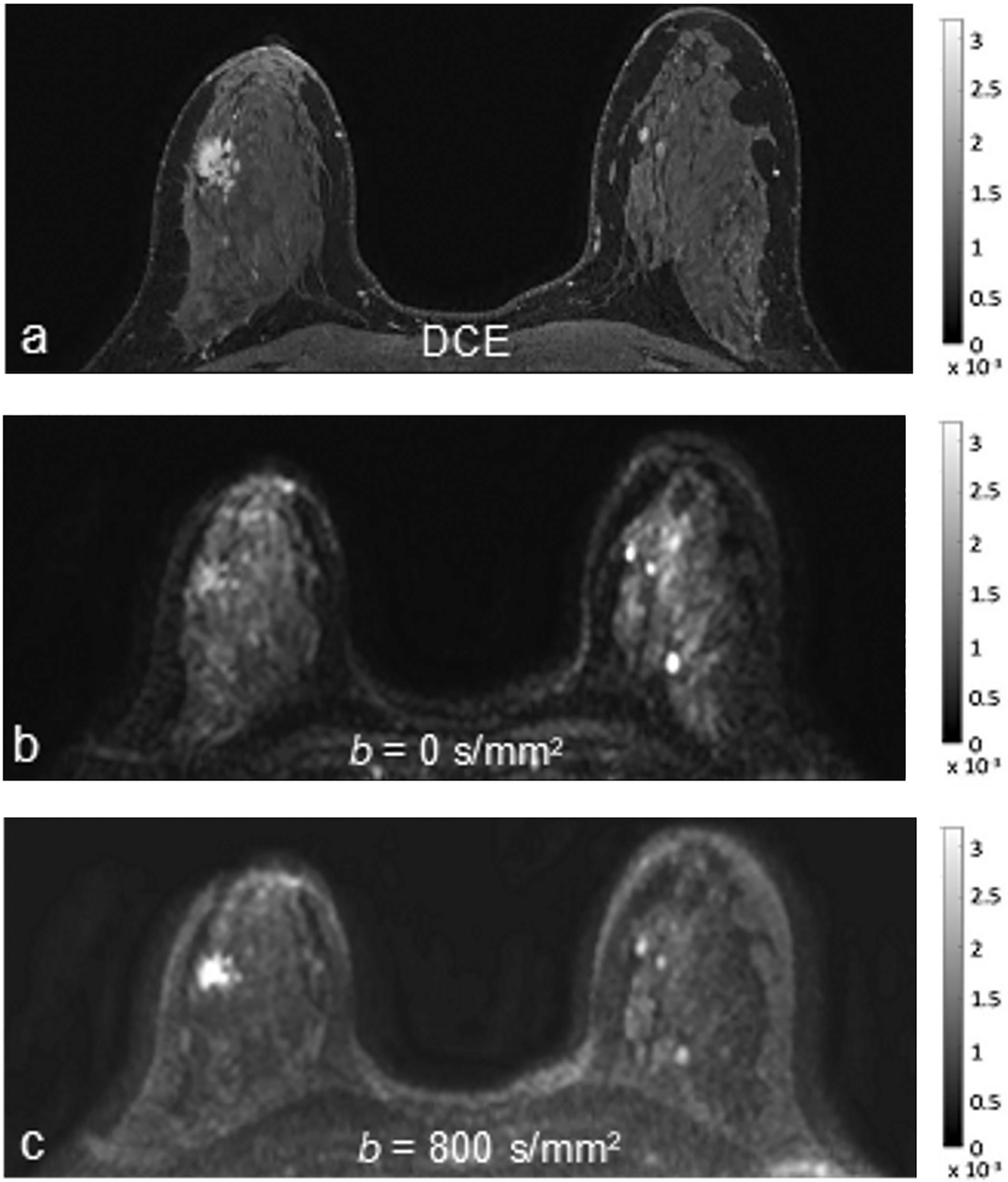

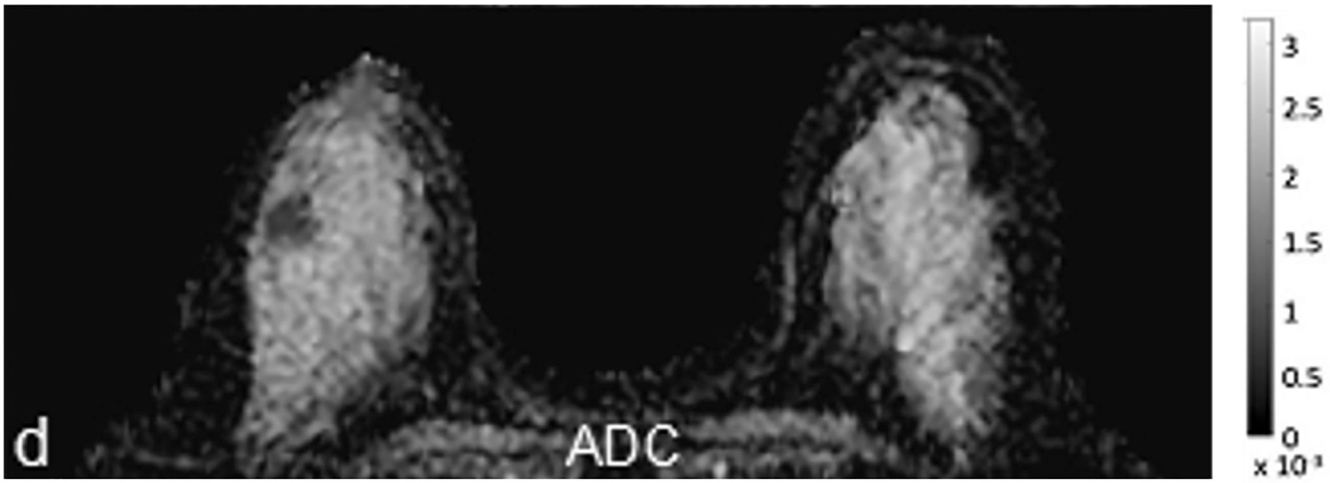

Fig 1—.

45-year-old woman with invasive ductal carcinoma, Nottingham grade 1, estrogen and progesterone receptor positive, and HER-2 negative. **(a)** DCE MRI shows 29-mm irregular enhancing mass (arrow) in upper outer quadrant of right breast. **(b)** DWI with $b = 0$ s/mm^2 shows isointensity of mass (arrow) compared to adjacent fibroglandular tissue. **(c)** DWI with $b = 800$ s/mm^2 shows hyperintensity of mass (arrow) compared to adjacent fibroglandular tissue. **(d)** $ADC_{0–800}$ map (calculated from acquired $b = 0$ and 800 s/mm^2 images) shows hypointensity of mass (arrow). ADC value of mass is 1.06×10^{-3} mm^2/s. DCE = dynamic contrast-enhanced

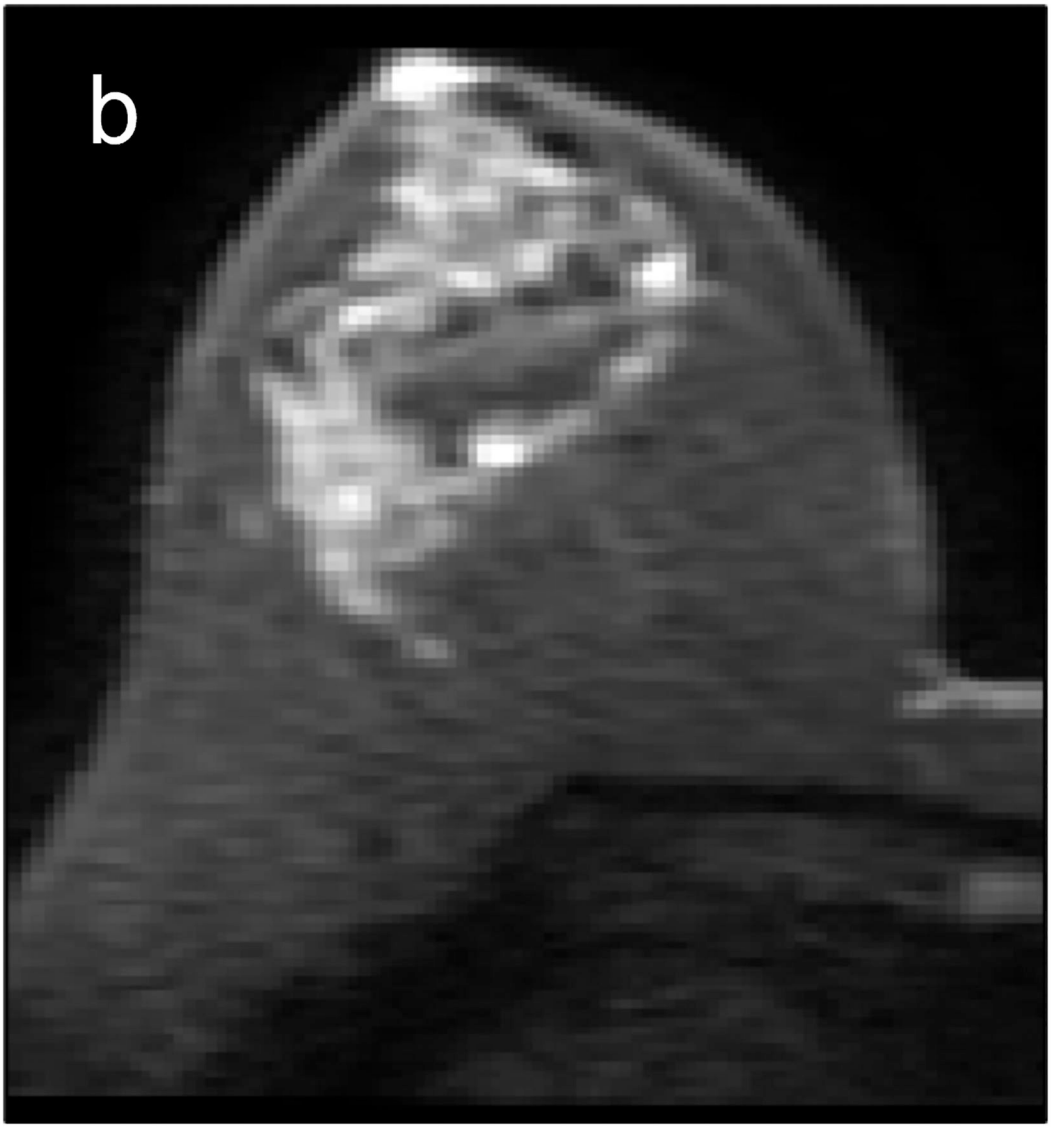

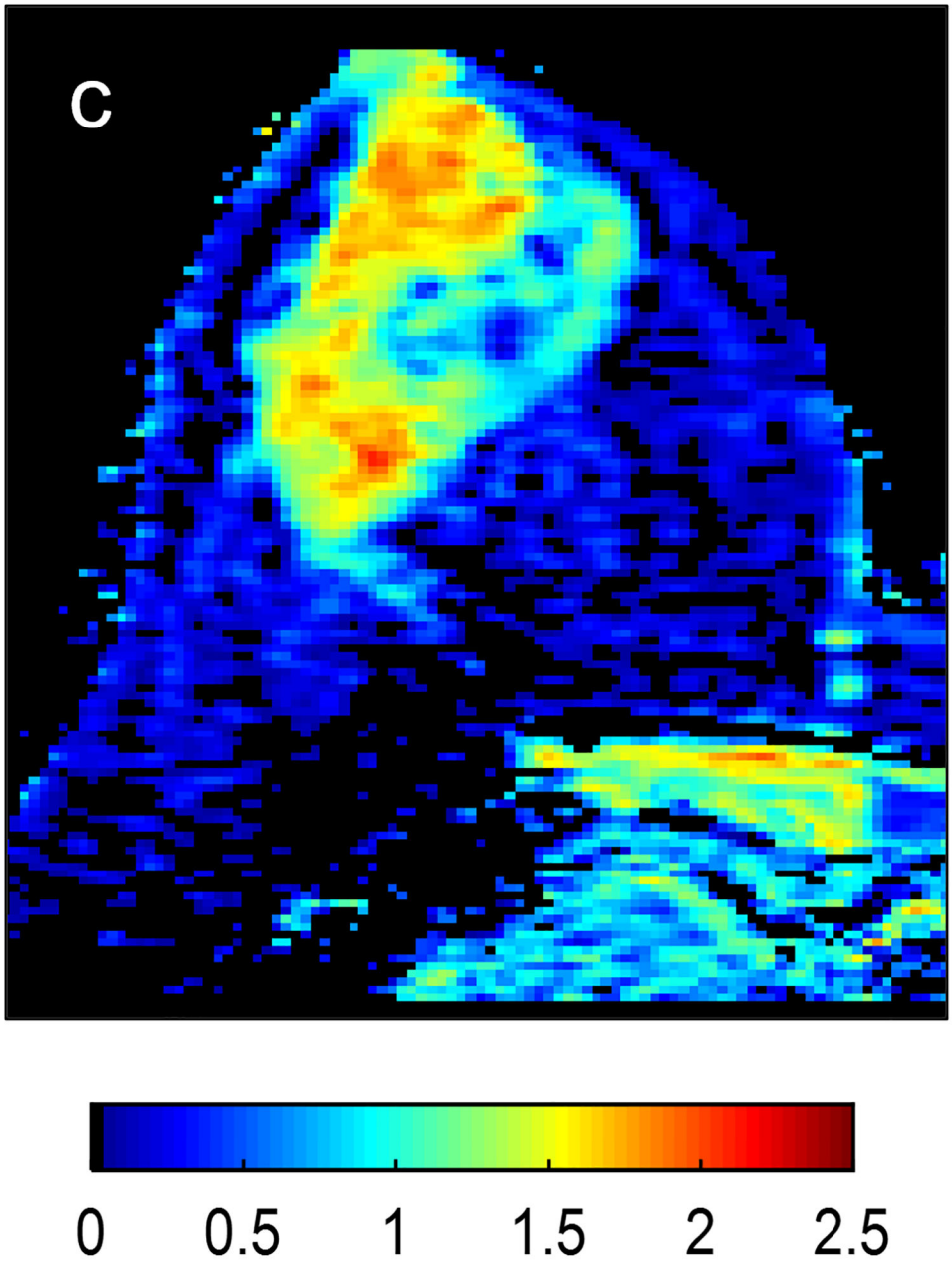

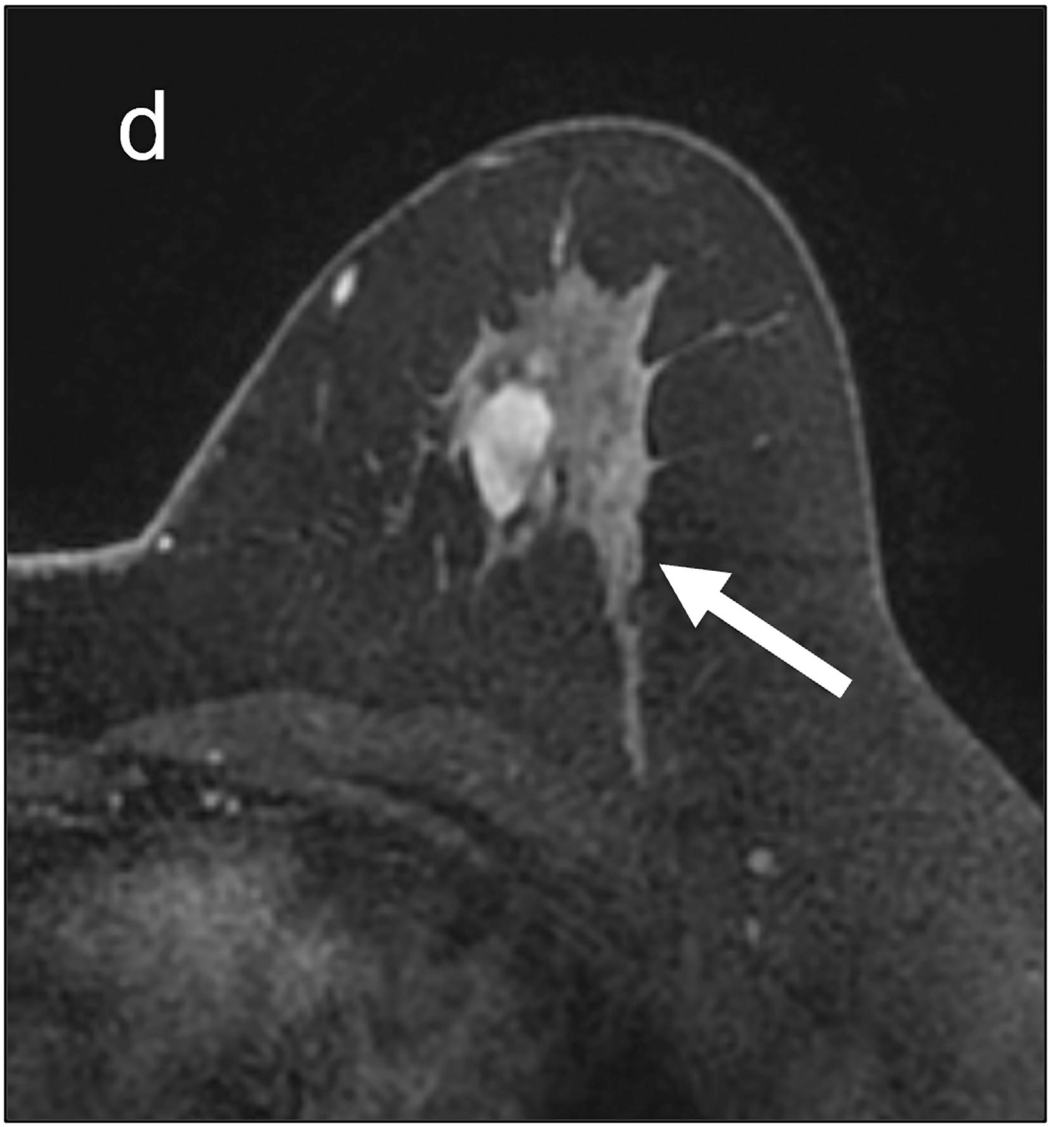

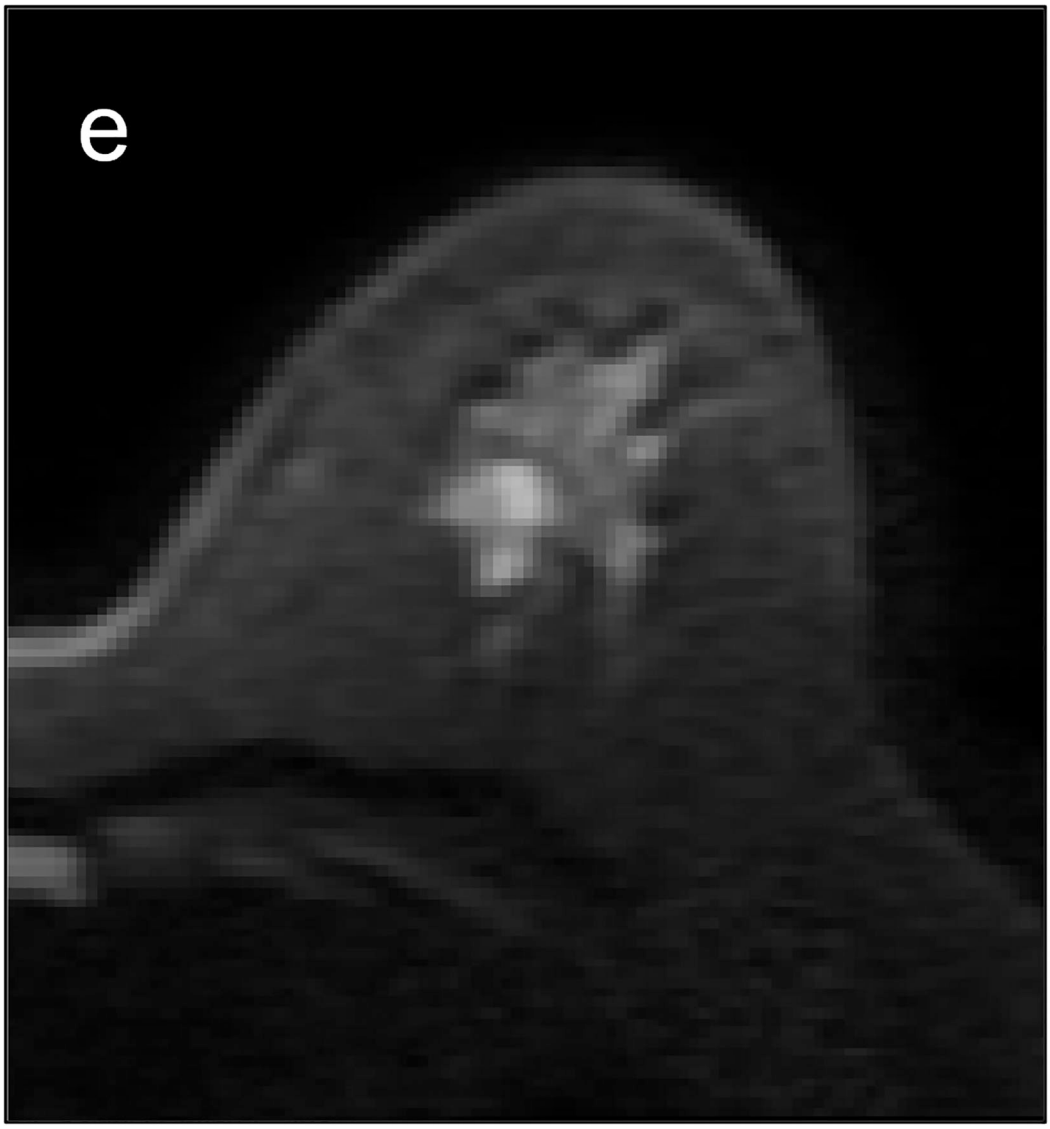

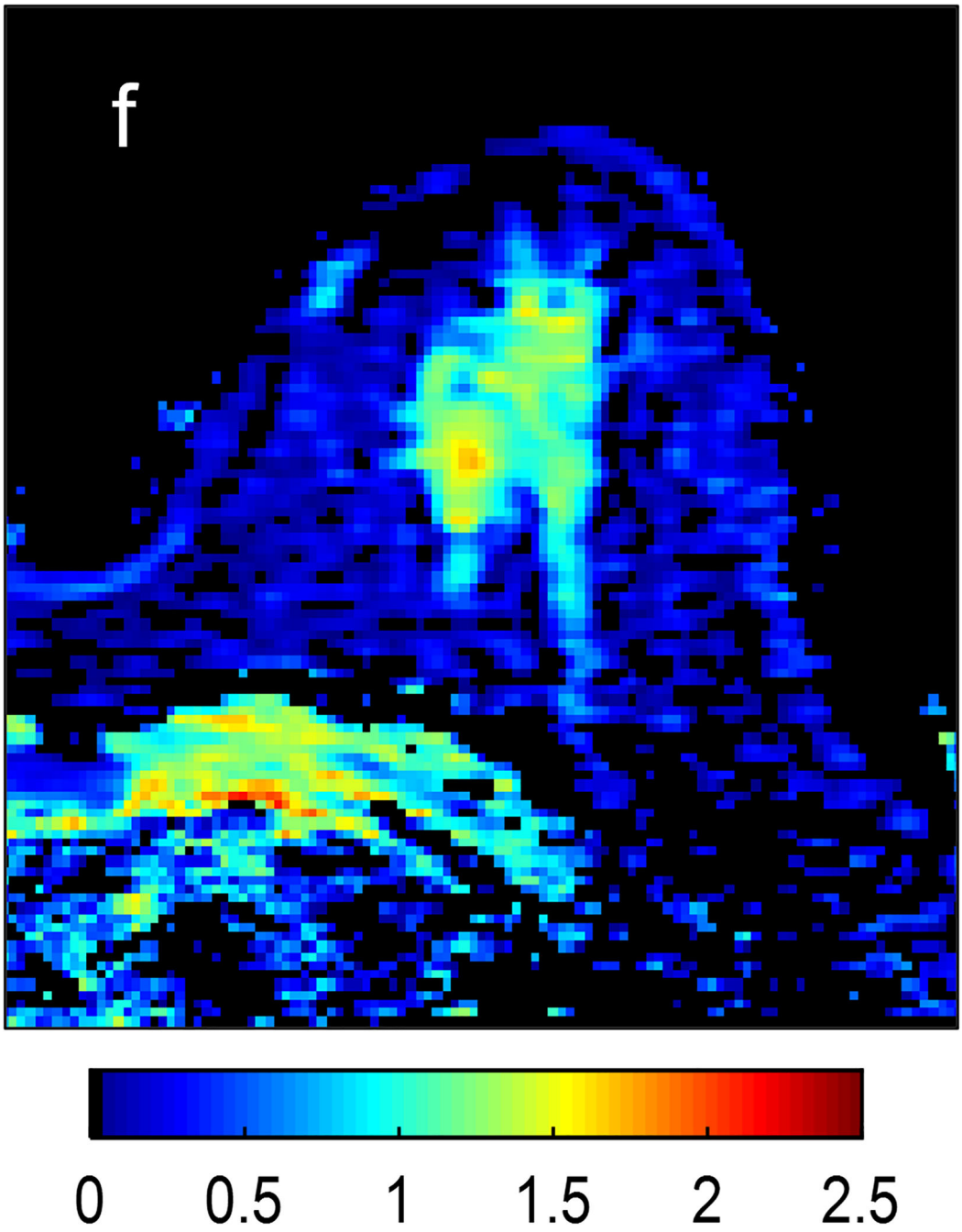

Fig 2—.

Two patients with benign breast lesions. (**a-c**) 49-year-old woman. **(a)** DCE MRI shows 48-mm non-mass enhancing lesion (arrow) in right breast **(b)** DWI shows no hindered diffusivity. **(c)** ADC map yielded $ADC_{0–800}$ value of $1.73 \times 10^{-3} mm^2/s$ for this lesion. Biopsy of lesion revealed columnar cell changes. (**d-f**) 42-year-old woman. **(d)** DCE MRI shows 19-mm enhancing lesion (arrow) in left breast. **(e)** DWI shows no hindered diffusivity. **(f)** ADC map yielded $ADC_{0–800}$ value of $1.56 \times 10^{-3} mm^2/s$ for this lesion. Biopsy of lesion revealed atypical ductal hyperplasia. Color bar aids interpretation of ADC values, whereby

blue indicates low ADC values and red indicates high ADC values. DCE = dynamic contrast-enhanced

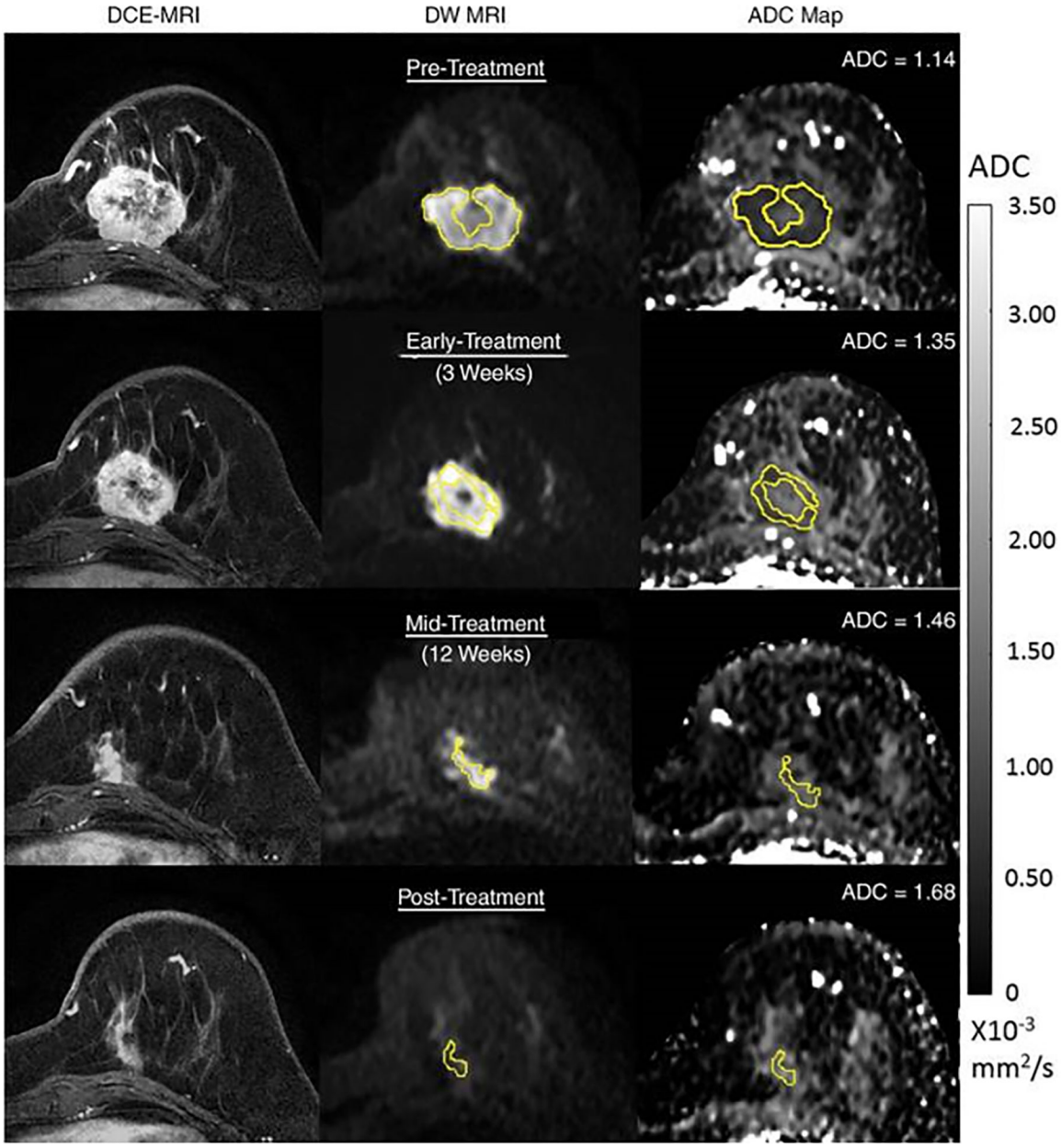

Fig 3—.

54-year-old woman with grade III triple-negative (hormone receptor–negative/human epidermal growth factor receptor 2–negative) breast cancer. Patient underwent neoadjuvant therapy. Serial 3-T MRI examinations were performed over course of treatment. DCE MRI (left), DWI (b = 800 sec/mm^2) (middle), and *ADC* map (right) before treatment (top row), during early treatment (after 3 weeks) (second row), during midtreatment (after 12 weeks) (third row), and after treatment (bottom row). Tumor measured 4.2 cm before treatment. At each time point, whole-tumor ROI was placed on multiple slices on DWI, avoiding central necrotic area, and mean ADC was calculated for all voxels in 3D ROI. ADC values increased progressively during treatment, yielding ΔADC = 18% at early treatment, 28% at midtreatment, and 47% at posttreatment. After treatment, patient was found to have

had pathologic complete response. Reprinted with permission from: Partridge SC, Zhang Z, Newitt DC, et al. Diffusion-weighted MRI Findings Predict Pathologic Response in Neoadjuvant Treatment of Breast Cancer: The ACRIN 6698 Multicenter Trial. *Radiology* 2018; 289:618–627.

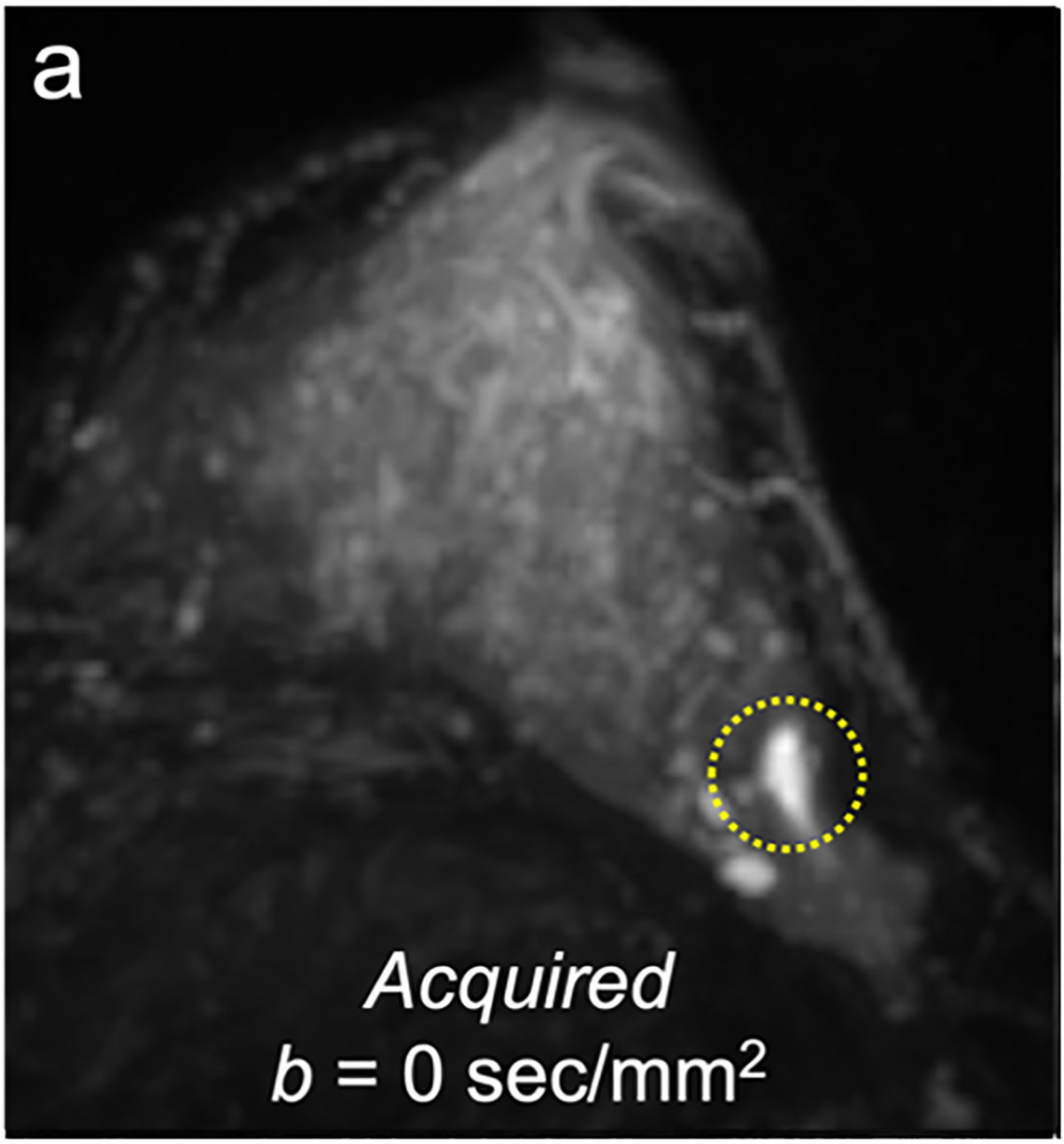

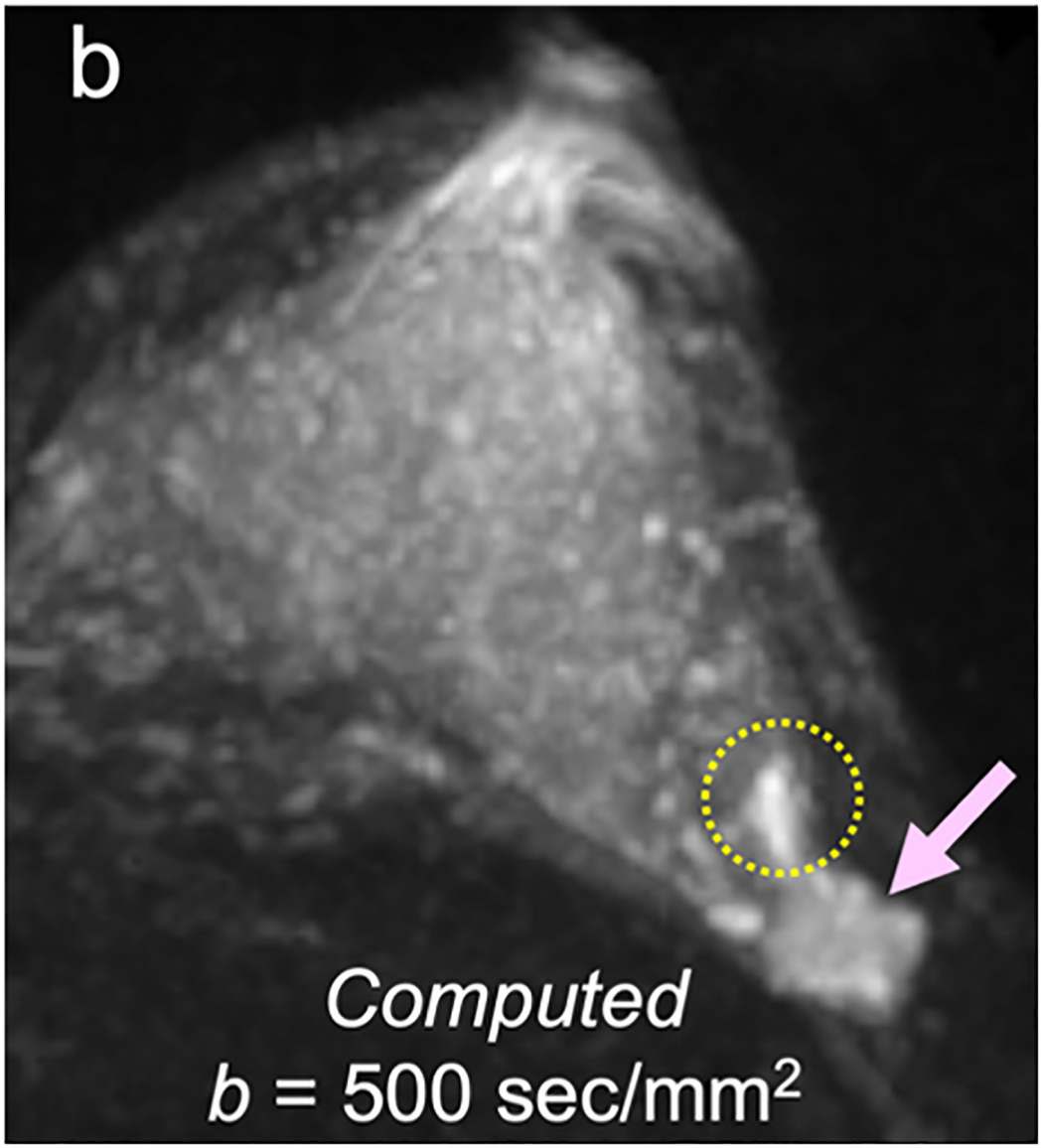

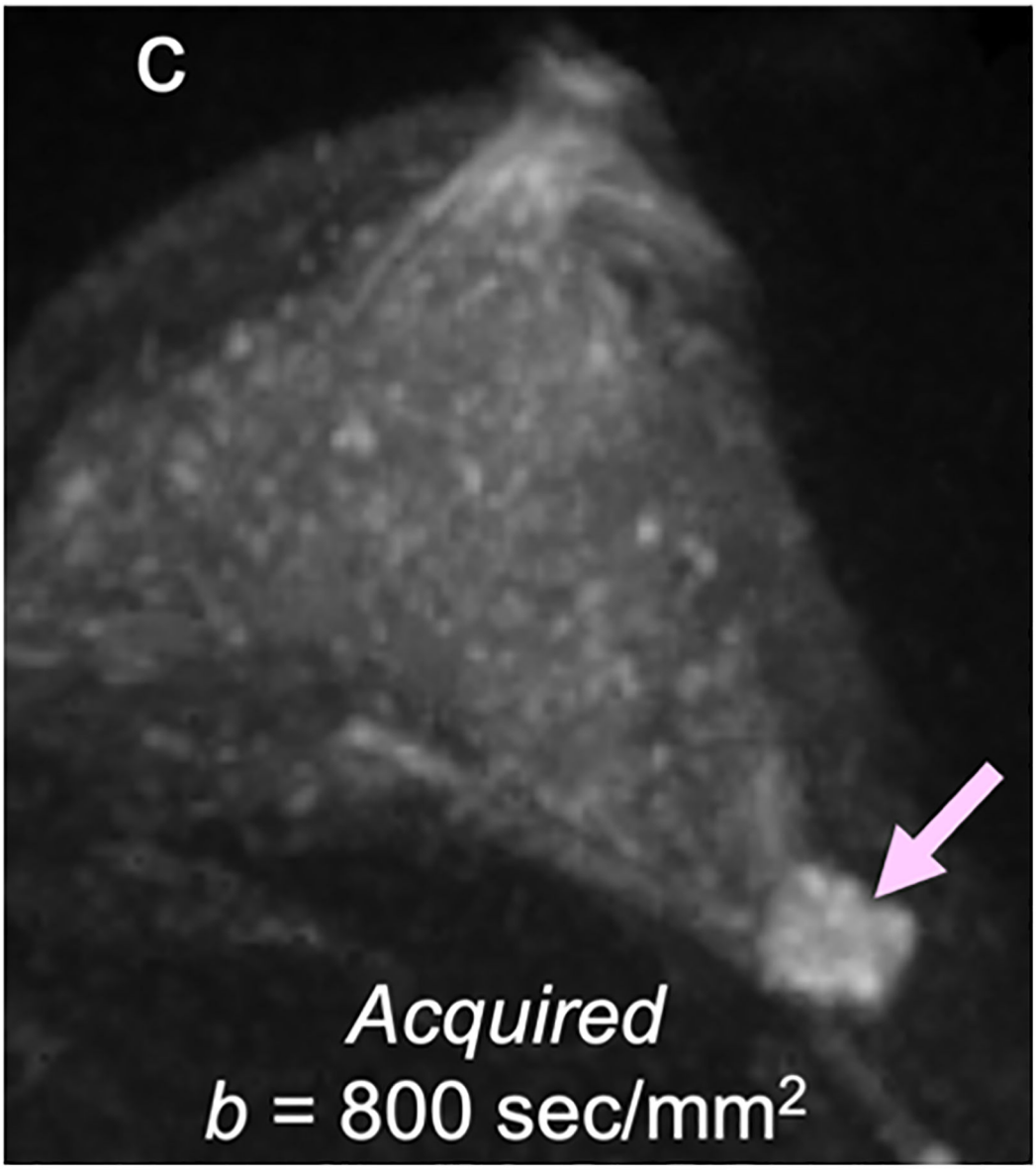

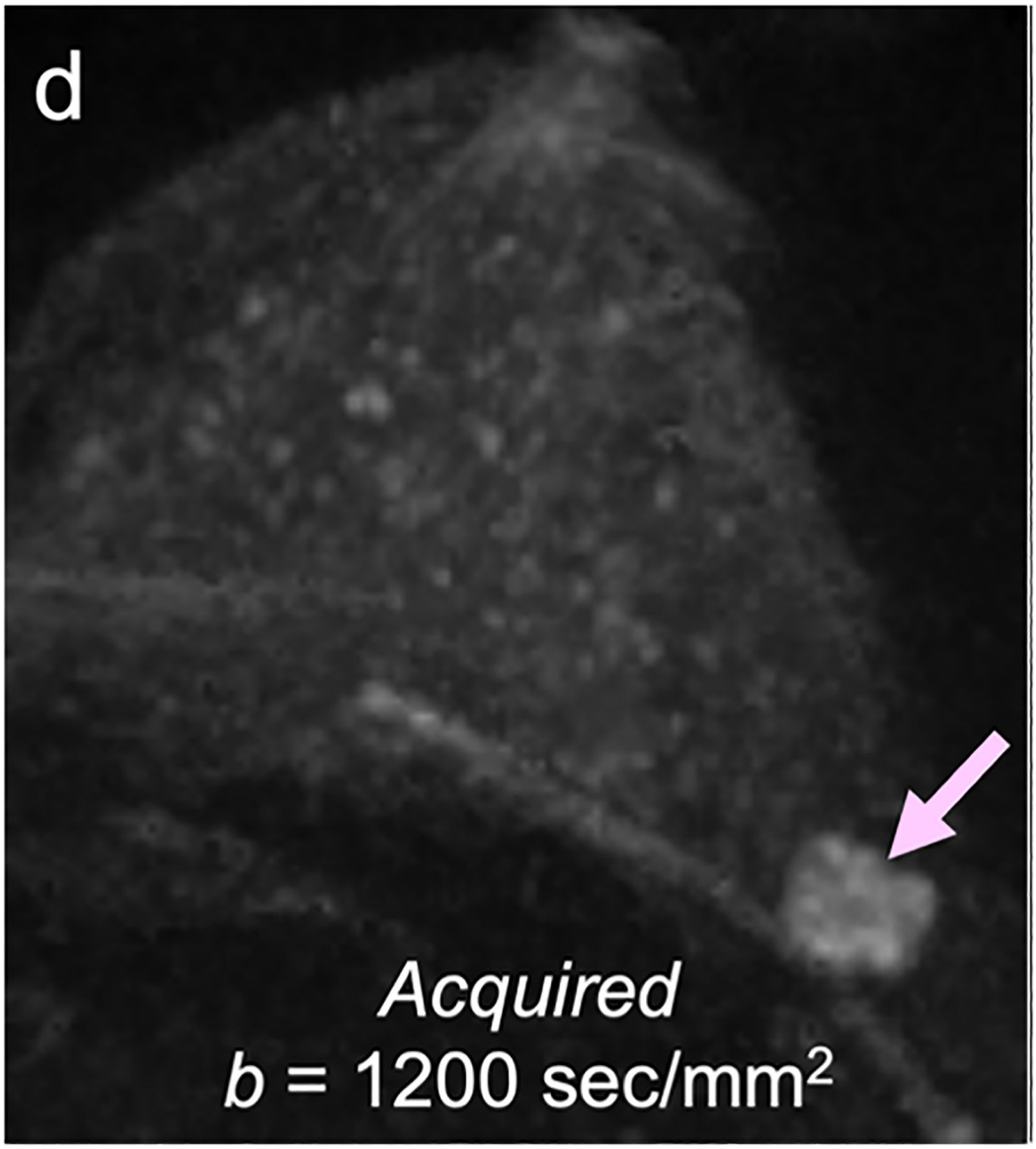

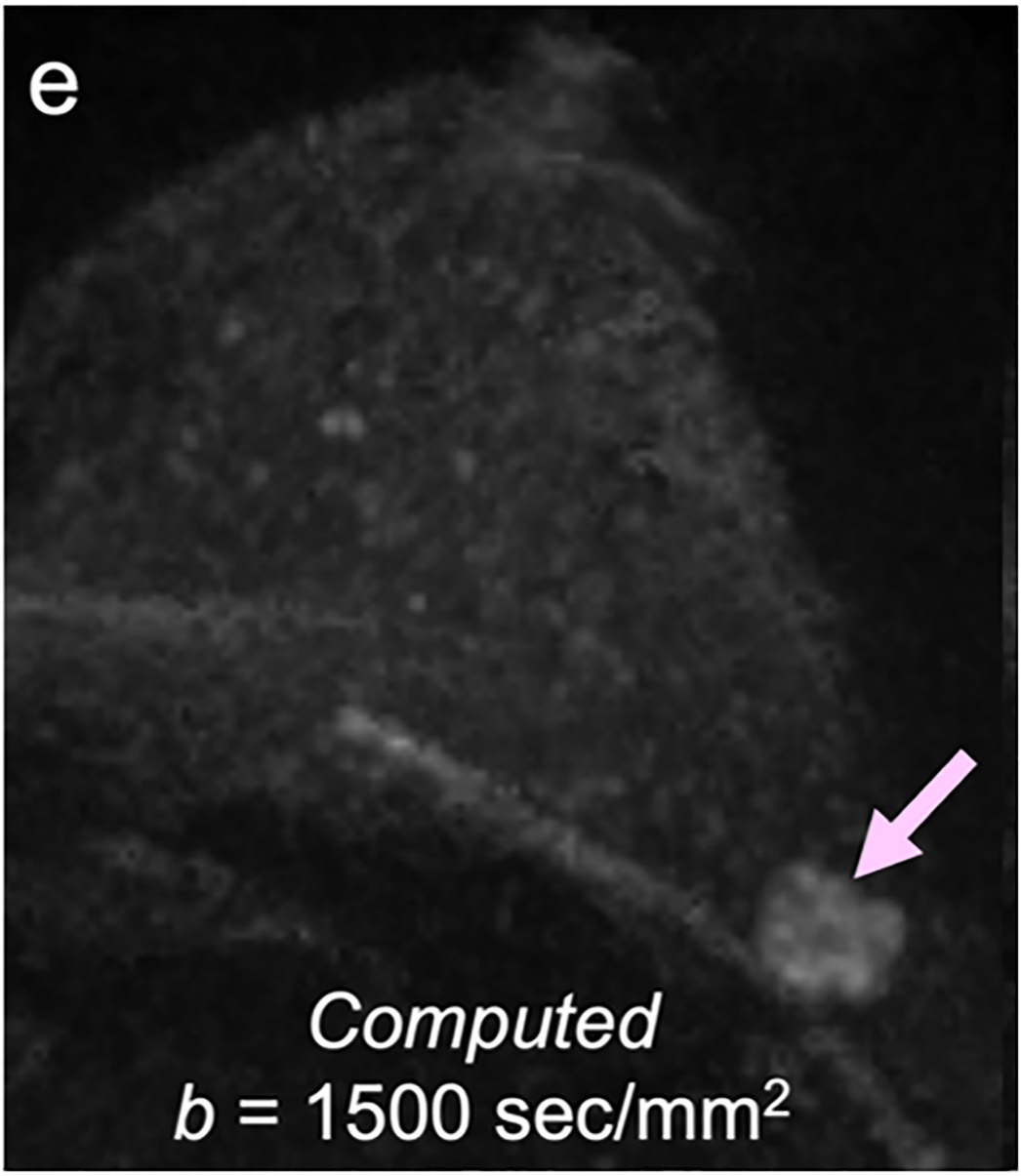

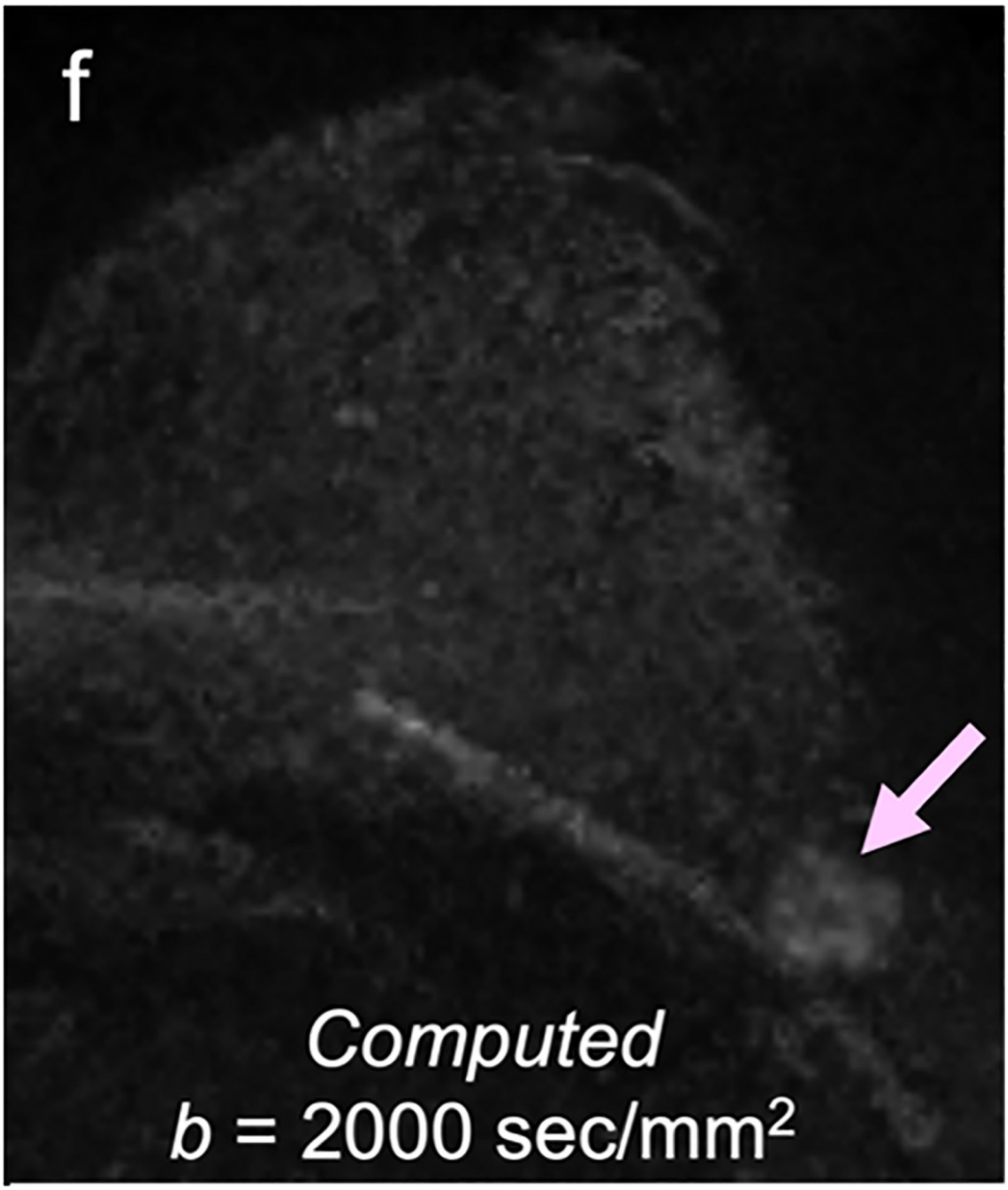

Fig 4—.

50-year-old woman with invasive cancer and adjacent cyst in upper outer quadrant of left breast. (**a**) DWI acquired with $b = 0$ s/mm^2 shows 10-mm high-signal-intensity mass (circle) in upper outer quadrant of breast (dashed circle). **(b)** DWI computed with $b = 500$ s/mm^2 shows decreased signal in mass (dashed circle). **(c)** DWI acquired with $b = 900$ s/mm^2 no longer shows hyperintensity in mass. $ADC_{0–800}$ value (calculated from acquired $b = 0$ and 800 s/mm^2 images) of this lesion was 2.56×10^{-3} mm^2/s, consistent with simple cyst. Images also show adjacent 15-mm mass in upper outer quadrant of breast (arrow, **b** and **c**). (**d**) DWI acquired with $b = 1200$ s/mm^2, (**e**) DWI computed with $b = 1500$ s/mm^2, and (**f**) DWI computed with $b = 2000$ s/mm^2 show increasing persistent hyperintensity in mass

(arrow, **d-f**). $ADC_{0–800}$ value (calculated from acquired $b = 0$ and 800 s/mm^2 images) of this lesion was 0.96×10^{-3} mm^2/s. Biopsy revealed lesion to be invasive ductal carcinoma.

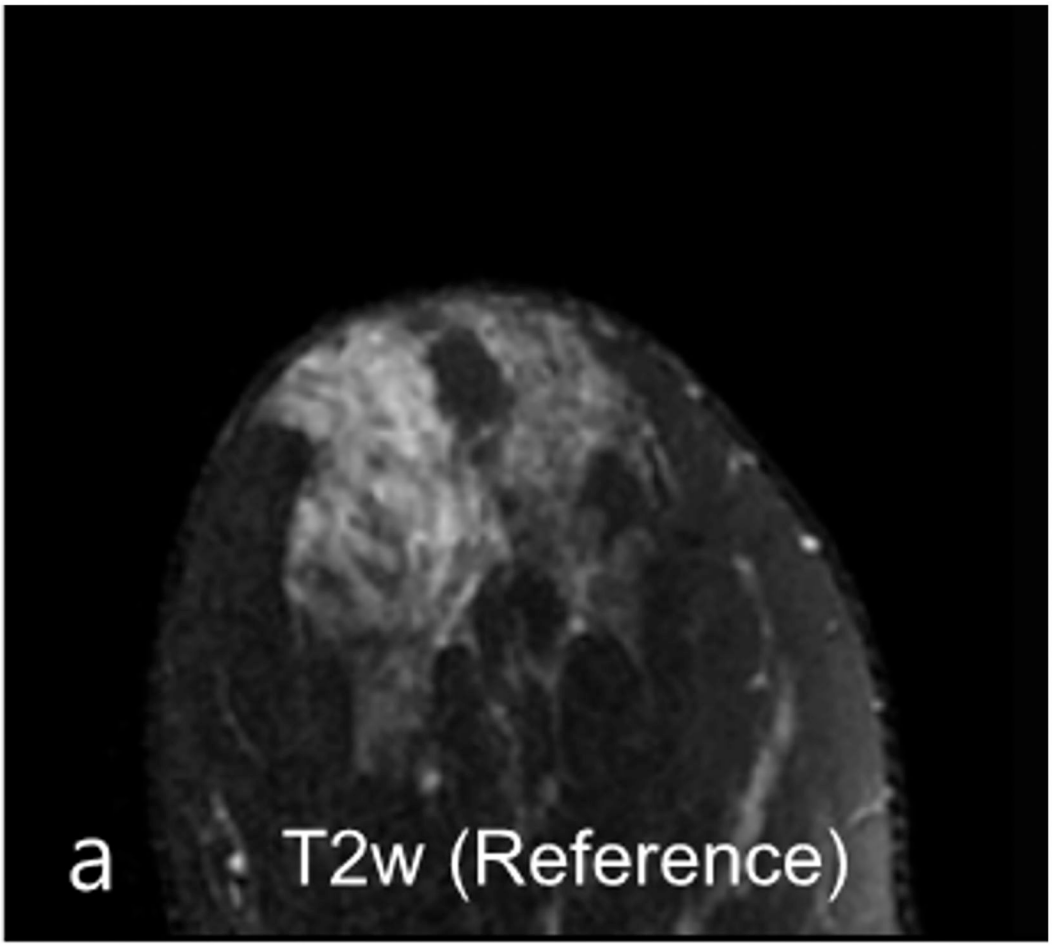

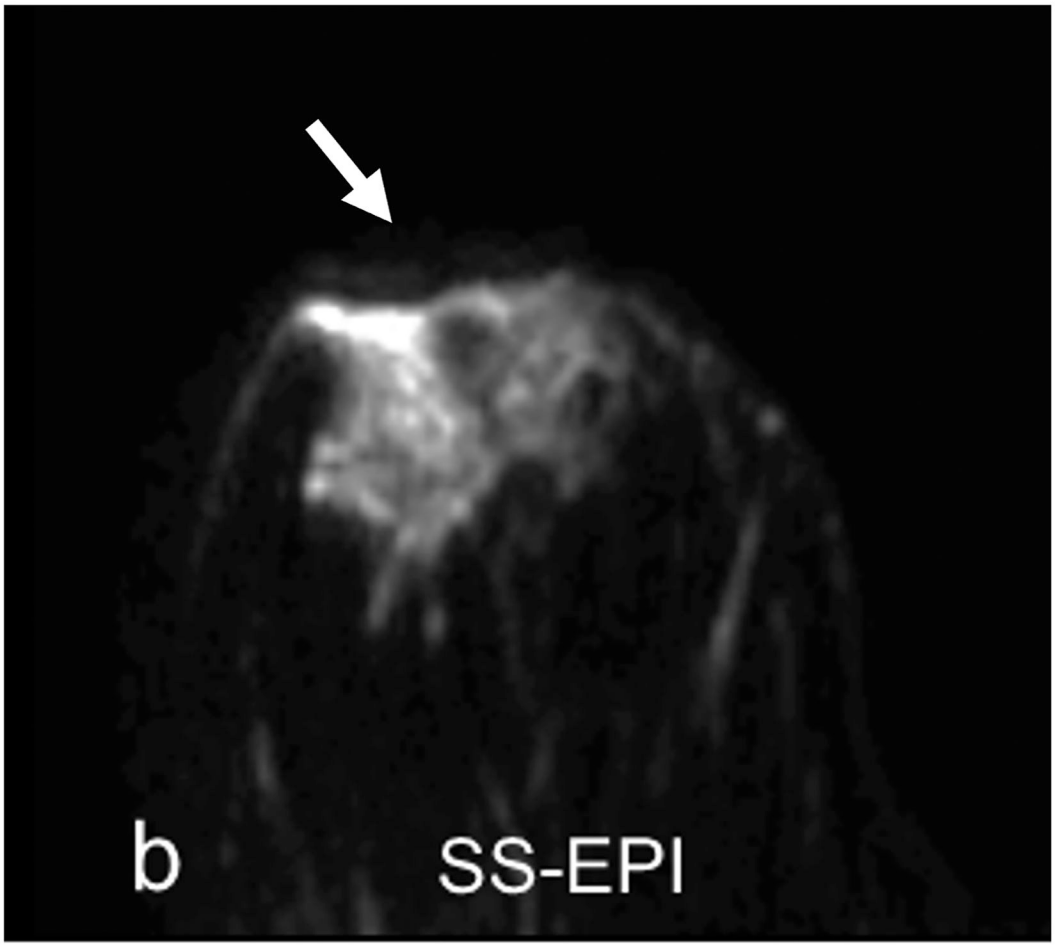

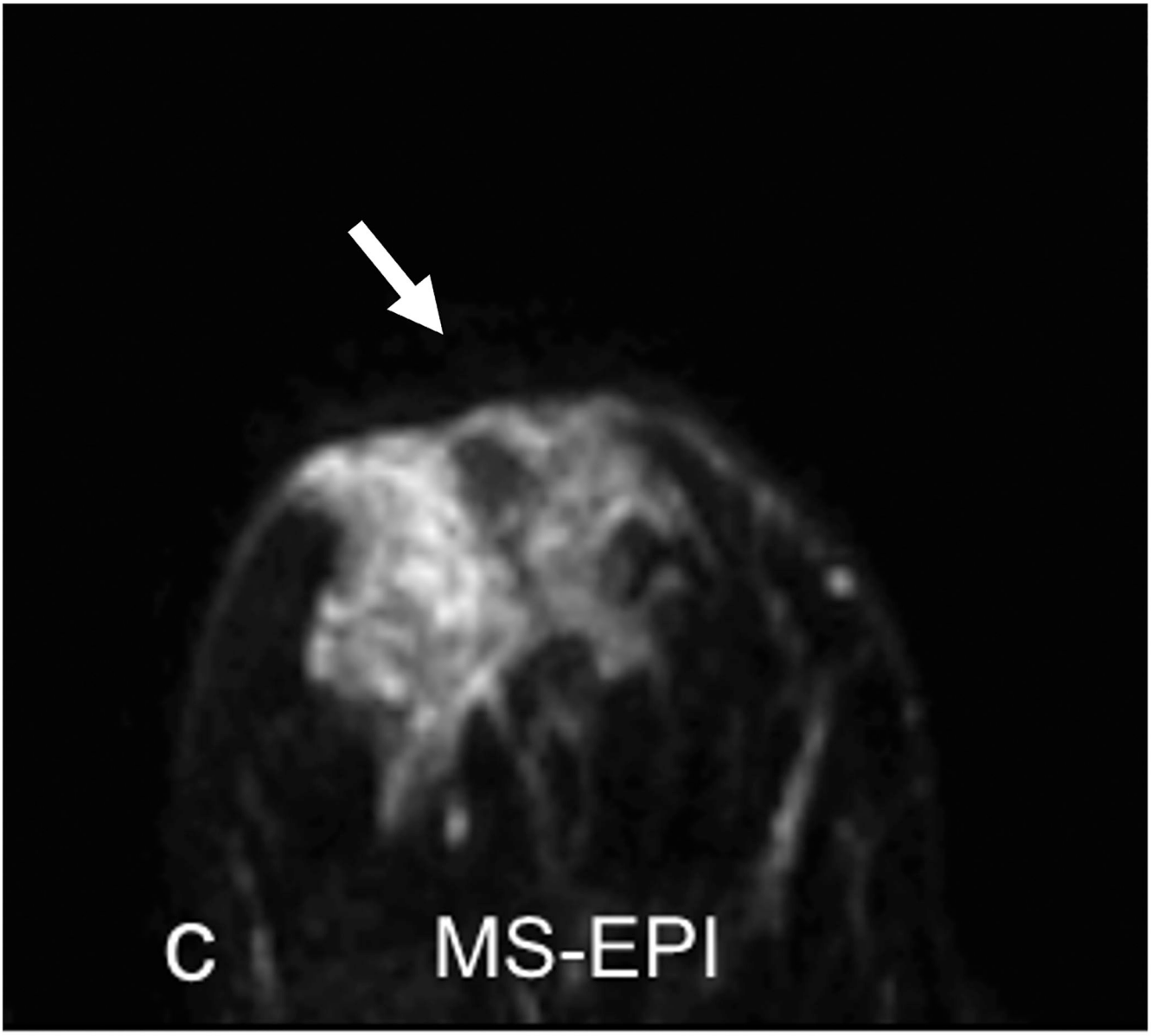

Fig 5—.

33-year-old woman undergoing high-risk screening by breast MRI. **(a)** T2-weighted fast spin-echo image (spatial resolution of 0.8 × 0. 8× 1.3 mm^3) serves as anatomic reference. **(b-c)** DWI with $b = 0$ s/mm^2 obtained using conventional single-shot echo-planar imaging (SS-EPI) (**b**), and using multi-shot EPI (**c**) (MS-EPI; Philips Healthcare IRIS technique, 2 shots), both with high spatial resolution of 1.2 × 1.2 × 4 mm^3. Distortions related to magnetic susceptibility effects in anterior breast (arrow, **b** and **c**) are reduced using MS-EPI acquisition compared to SS-EPI acquisition. Examination shows no suspicious breast findings.

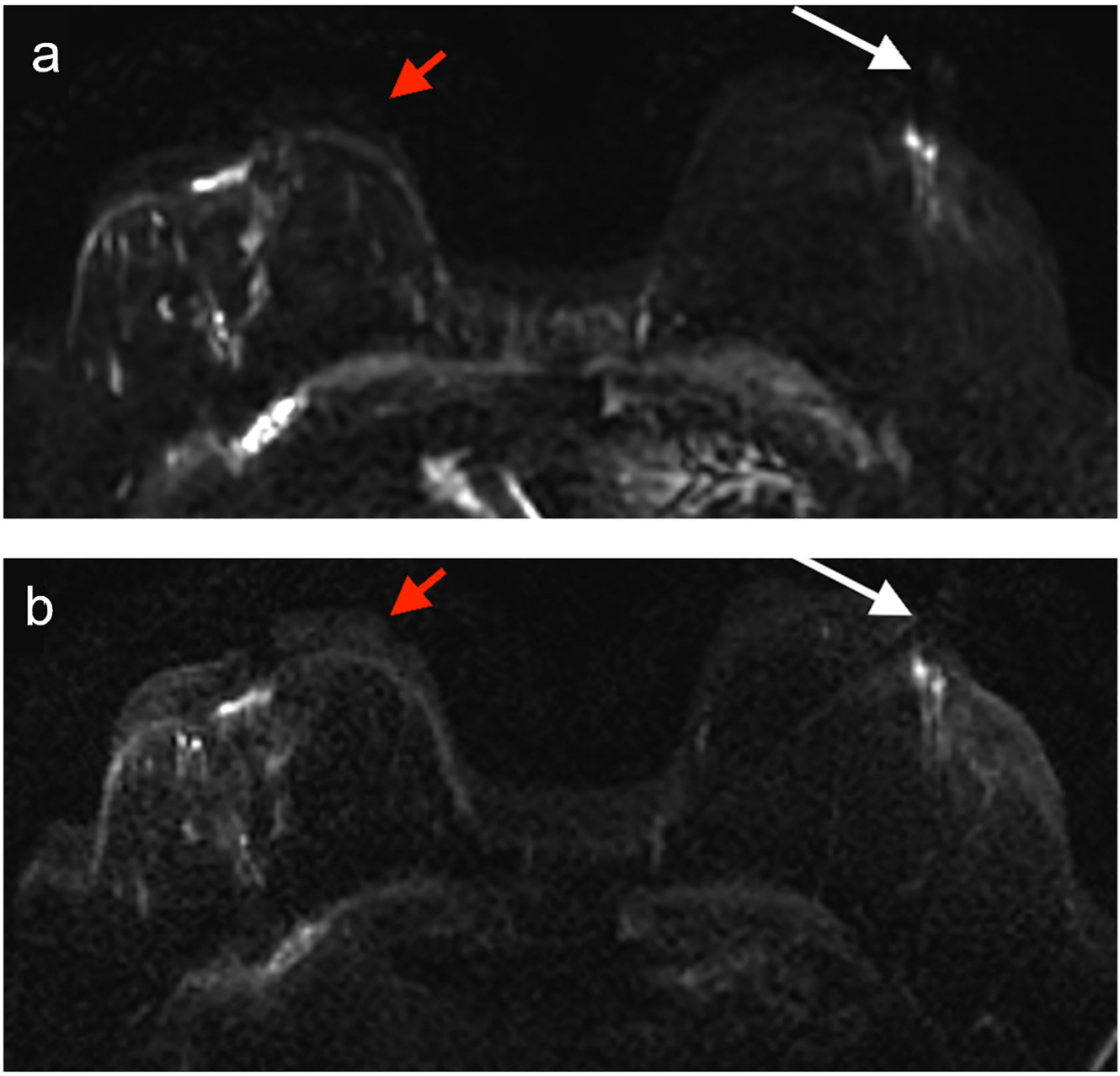

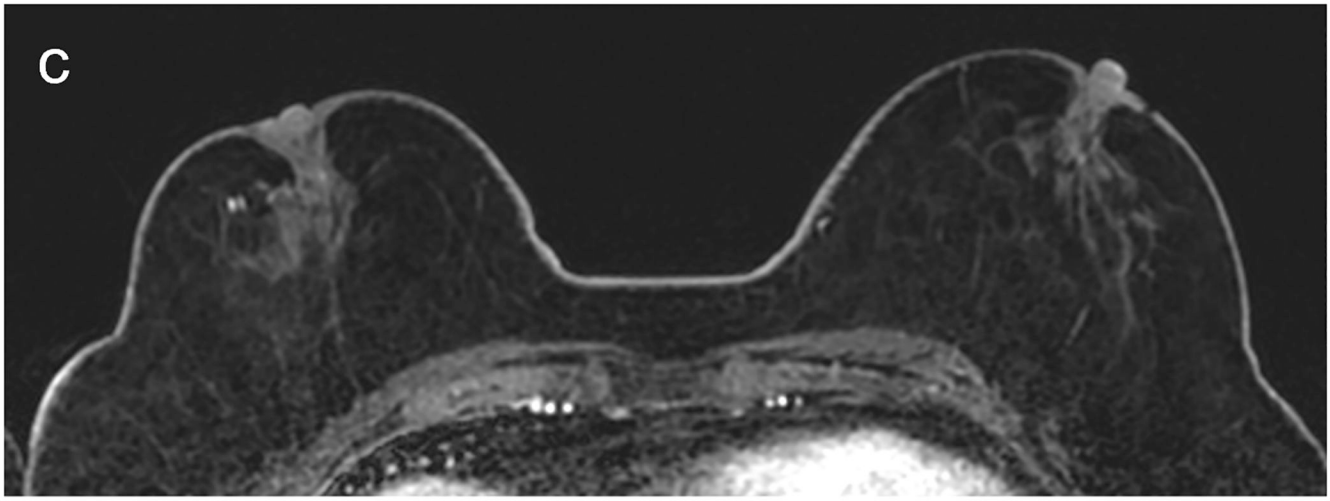

Fig 6—.

50X-year-old patient undergoing surveillance MRI. **(a)** DWI with deep learning reconstruction, **(b)** DWI with standard single-shot technique, and **(c)** contrast-enhanced T1-weighted image show post-surgical changes in right breast and no suspicious findings. DWI with deep learning reconstruction shows better image quality than DWI with standard singe-shot technique, including improved visibility of skin, decreased artifact (white arrow, **a** and **b**), and improved visibility of left nipple (red arrow, **a** and **b**). DWI with deep learning reconstruction also appears less grainy compared to standard single-shot DWI. Case illustrates use of novel AI-enhanced DWI reconstruction technique to aid image denoising, to allow improved image quality and improved spatial resolution. AI = artificial intelligence